

ABSTRACT

Title of Thesis : **THE EFFECT OF DEAD, LIVE AND BLAST LOADS ON A SUSPENSION BRIDGE**

Kunal N. Suthar, Master of Science, 2007

Thesis directed by : Dr. Chung C. Fu
 Department of Civil and Environmental Engineering

Bridges in America are of special importance. The analysis of these bridges should be carried out for different loading conditions. Bridges are normally designed for dead load, live load and other occasional loads. American Association of State Highways and Transportation Officials (AASHTO) have specified for the ship impact, seismic vulnerability and also against vehicular collisions. But there are no definite structural design criteria for the bridges under typical blast loadings.

This thesis is intended to provide a basic guideline for using the blast load analysis on the suspension bridge. Further research may be carried out in this field to develop some standards for the bridge resistance against explosions. Also, the AASHTO loading was applied to study the effect of live load on the bridge. The results obtained from live loading on the same suspension bridge were implemented to allocate costs depending upon the effect of particular vehicle on the bridge deck.

To study the non-linear analysis, a three-dimensional finite analysis model under dynamic load has been established for the Suspension bridge part (West-bound side) of the Chesapeake Bay Bridge for determining the effect of live load, which was used for cost allocation studies. This vehicle-bridge interaction modeling was done using a Finite Element Software known as “Visual Bridge Design System” (VBDS). Development and interaction of a detailed truck using proper design standards were applied to realistically represent the actual loading conditions. The results obtained were in close proximity

when compared with the data available through the State Road Commission, State of Maryland. Results presented in this thesis hence demonstrate a significant potential for using the VBDS and for thorough investigation of the vehicle-bridge interaction and dynamic loading on bridges.

For carrying out the impact of blast loading, the bridge was modeled in parallel using the SAP2000 system. The whole modeling of the suspension part of the bay bridge was done on the SAP2000 for carrying out the non-linear analysis of the blast loads. The behaviors of each element under the effect of the blasts were studied from the output generated by the SAP2000. The output of the software presents results including moments, axial loads and displacements. Moreover, moments and axial load at each node and at any point within the element, can be easily obtained from the software output. The “progressive collapse” approach of the bridge was also carried out to know the exact behavior with the formation of the plastic hinges under the impact of blast loadings. Also the comparisons of the blast loads with and without the application of initial stress were carried out. This shows the importance of using initial stress in the analysis of a suspension bridge.

**THE EFFECT OF DEAD, LIVE AND BLAST LOADS ON A
SUSPENSION BRIDGE**

By

Kunal Suthar

Thesis submitted to the Faculty of the Graduate School of the
University of Maryland, College Park, in partial fulfillment
of the requirements for the degree of
Master of Science
2007

Advisory Committee:

Dr. Chung C. Fu (Chair)

Dr. M. Sherif Aggour

Dr. Amde M. Amde

© Copyright by
Kunal N. Suthar
2007

ACKNOWLEDGMENTS

Firstly, I would like to express a huge sense of gratitude towards my advisor, Dr. C.C. Fu, for all his help in preparing this thesis, and for serving on the advisory committee. I am very grateful for all the expertise he shared with me and all the opportunities he has afforded me. I truly appreciate his guidance, which has provided me with ample knowledge.

I would like to thank Dr. Shuqing Wang for the valuable inputs he has provided during the development of the mathematical model, who took time out to instill intellectual advice and strode me through the right path.

I would also like to thank Dr. Amde and Dr. Aggour for serving on the advisory committee and going through my work, inspite of a busy schedule.

Finally, but far from least, I would like to thank my fellow research assistants of the Civil Engineering Department, my family especially my brother Vishal Suthar, Mehul Dave and Jagannath Chakravarty for their relentless support throughout the course of this thesis, without whom this wouldn't have been possible.

TABLE OF CONTENTS

LIST OF FIGURES -----	v
LIST OF TABLES -----	vii
1. INTRODUCTION-----	1
1.1. Problem statement-----	1
1.2. Description of the Model Bridge -----	1
2. SUSPENSION BRIDGE -----	3
2.1. Historic Background -----	3
2.2. Components of Suspension bridge -----	3
2.3. Economic proportions for suspension bridges-----	7
2.4. Theories of Suspension Bridges-----	9
<i>2.4.1 Rankine's Theory:-</i> -----	9
2.4.1.1. The Two-pinned Girder with a Single Concentrated Load: -----	11
<i>2.4.2 The Elastic Theory:</i> -----	14
2.4.2.1 Temperature Effects: -----	14
<i>2.4.3 Deflection Theory</i> -----	16
2.4.3.1 Basic Equations: -----	17
<i>2.4.4 The Linearised Deflection Theory</i> -----	19
3. DEAD LOAD, LIVE LOAD & BLAST LOADS-----	21
3.1 Dead load -----	21
3.2 Vehicular Live Load-----	21
3.3 Blast Load-----	22
<i>3.3.1 Equivalent Static Loads</i> -----	23
<i>3.3.2 Comparison of Blast loads and Seismic Loading:</i> -----	27
4. SUSPENSION BRIDGE IMPLEMENTATION-----	31
4.1 VBDS-----	31
4.2 SAP2000 Software-----	32
4.3 Bridge Model -----	34
<i>4.3.1 VBDS Bridge Model</i> -----	35
<i>4.3.2 SAP2000 Bridge Model</i> -----	38

5. BLAST LOAD CASES-----	40
5.1 Load Combination 1 -----	41
5.2 Load Combination 2 -----	44
5.3 Load Combination 3 -----	46
5.4 Progressive Collapse-----	48
6. CONCLUSION-----	62
APPENDIX -----	64
REFERENCE-----	80

LIST OF FIGURES

Figure 1.1- William Preston Lane, Jr. Memorial Bridge	2
Figure 2.1- Members of a suspension bridge	4
Figure 2.2- Tower of suspension bridge (Golden Gate Bridge, SF).....	5
Figure 2.3- Stiffening girder supported by a cable through hangers	9
Figure 2.4- Shear and Bending Moment Diagrams for a single concentrated load.....	12
Figure 2.5- Influence lines for bending moment and shear forces in the stiffening girder...	13
Figure 2.6- Comparison between different theories (Pugsley, A.)	19
Figure 3.1 Variation of pressure from distance of explosion.....	25
Figure 3.2- Blast pressure distribution on bridge deck (elevation)	26
Figure 3.3 Blast pressure distributions on bridge deck (plan)	26
Figure 3.4- Comparison of blast and seismic actions on structures	29
Figure 4.1- Bridge model in VBDS	37
Figure 4.2- Live load analysis model in VBDS	38
Figure 4.3- Bridge model in SAP2000	39
Figure 5.1- Application of Blast load at centre of mid-span.....	41
Figure 5.2- Axial force diagram for blast load case 1	42
Figure 5.3- Bending moment diagram for blast load case 1	43
Figure 5.4- Bending moment diagram for blast load case 1	43
Figure 5.5- Application of Blast load at centre of side-span	45
Figure 5.6- Axial force diagram for blast load case 2.....	45
Figure 5.7- Bending moment diagram for blast load case 2	46
Figure 5.8- Application of Blast load at end of mid-span.....	47
Figure 5.9- Axial force diagram for blast load case 3.....	47
Figure 5.10- Bending moment diagram for blast load case 3	48
Figure 5.11- Curve showing relationship between force and deformation.....	50
Figure 5.12- Plastic hinge properties in SAP2000.....	52
Figure 5.13- Formation of Plastic Hinges due to blast load 1 (step 1)	53

Figure 5.14- Formation of Plastic Hinges due to blast load 1 (step 1)	53
Figure 5.15- Formation of Plastic Hinges due to blast load 1 (step 3)	54
Figure 5.16- Formation of Plastic Hinges due to blast load 1 (step 5)	54
Figure 5.17- Formation of Plastic Hinges due to blast load 1 (step 12)	55
Figure 5.18- Formation of Plastic Hinges due to blast load 1 (step 18)	55
Figure 5.19- Formation of Plastic Hinges due to blast load 2 (step 1)	56
Figure 5.20- Formation of Plastic Hinges due to blast load 2 (step 5)	56
Figure 5.21- Formation of Plastic Hinges due to blast load 2 (step 11)	57
Figure 5.22- Formation of Plastic Hinges due to blast load 3 (step 1)	57
Figure 5.23- Formation of Plastic Hinges due to blast load 3 (step 5)	58
Figure 5.24- Formation of Plastic Hinges due to blast load 3 (step 10)	58
Figure 5.25- Relationship between plastic deformation Vs axial loads (step 0)	59
Figure 5.26- Relationship between plastic deformation Vs axial loads (step 8)	59
Figure 5.27- Relationship between plastic deformation Vs axial loads (step 11)	60
Figure 5.28- Relationship between plastic deformation Vs axial loads (step 13)	60

LIST OF TABLES

Table 3.1- Equivalent Static Parameters for 500 lb of TNT Explosion.....	24
Table 3.2- Summary of Seismic loading and the Blast loading Differences	28
Table 4.1- Description of different sub components of the bridge model	36
Table 5.1- Material property	36
Table 5.1- Load Cases.....	40
Table 5.2- Results for Plastic hinge located at node 942	51
Table 5.3- Effects of the initial stress on the deflection of the bridge.....	61
Table 5.1- Max vertical displacements due to application of blast loads combination (1.25 DL + 0.5LL + 1.0 BLAST).....	61

1. INTRODUCTION

Bridge response induced by moving vehicles is an important aspect in the design and structural evaluation of bridges. There are quite some phenomena that influence the bridge's behavior. For the better understanding of the suspension bridge, different theories have been discussed here like, The Rankine Theory, The Elastic Theory, The Deflection Theory, and also The Linearized Deflection Theory.

1.1. Problem statement

American Association of State Highways and Transportation Officials (AASHTO) have design methodologies for the ship impact, seismic vulnerability and also against vehicular collisions. But there are no definite structural design criteria for the bridges under typical blast loadings.

The intent of this research is to carry out the dead, live and blast load analysis on a suspension part of William Preston lane Jr. Memorial Bridge. The dead and live load analysis that was carried out on VBDS was further used for cost allocation studies. Loading was applied in the form of HS-20 truck and corresponding effects for different loading trucks were calculated. The blast loads analysis was carried out on SAP2000 to check the bridge vulnerability against explosions. Depending upon this research, further standard can be defined for the suspension bridge to resist the impact of blast loads.

1.2. Description of the Model Bridge

The Chesapeake Bay Bridge, also simply known as the Bay Bridge (officially known as William Preston Lane, Jr. Memorial Bridge) is located in Maryland, which spans the Chesapeake Bay and connects the state's Eastern and Western Shore regions of Maryland. The bridge actually comprises of two bridge bounds, namely, the east bound bridge and the west bound bridge, the former was built in 1952, while the latter was built in 1973.



Figure 1.1.William Preston Lane, Jr. Memorial Bridge

With the total length of 4.33 and 4.35 miles, the bridges are the longest in the state of Maryland and are also among the world's longest and most-scenic over-water structures. The center suspension span on the east bound bridge is 1600 feet in length with a maximum clearance of 186 feet. The side spans are of 675 feet. The maximum elevation for the cables is about 177.73 feet.

2. SUSPENSION BRIDGE

2.1. Historic Background

The idea of suspension bridge was first suggested by nature to the extravagancies of ropes of creepers, vines and other trailing plants in the warm countries. It was a bridge created by primitive man, found in South East Asia, South America and Equatorial Africa. The translation of these elementary suspension bridges built of natural ropes into terms of metal occurred first in China. The ropes were replaced with iron chains and towers were built mainly of masonry. With this introduction of wrought iron, western people showed their interest and built the first chain bridge in England in 1741. Later, the influence of use of suspension bridge increased and first credited iron suspension bridge was built in Pennsylvania in 1796.

With the passage of time, the principal of uniform stresses throughout the spans and increasing stiffness by means of deck girders become more popular. Later, Rankine produced his approximate theory for two or three hinged stiffening girders that has been used so much ever since. With the completion of Brooklyn Bridge, there came two major steps in the theory of suspension bridges – “elastic” and “deflection” theories. Alongside, there was much revision made in the deflection theory to make it more and more accurate.

2.2. Components of Suspension bridge

A suspension bridge is mainly divided into two categories, superstructure and substructure. Bridge deck, cables, hangers, main supporting system, lateral bracing and tower (above bridge deck) are included in superstructure, whereas foundation, anchorages, pier caps and columns falls under substructure.

The normal order for the erection of suspension bridge is: substructure, towers and anchorages, footbridges, cables, suspenders, stiffening truss and floor system, roadway

and cable wrapping. The erection of suspension bridge is comparatively simple, and is also free from dangers attending other types of long span constructions. The towers of the suspension bridge are in compression whereas the cables and hangers are the members in compression as shown in Figure 2.1.

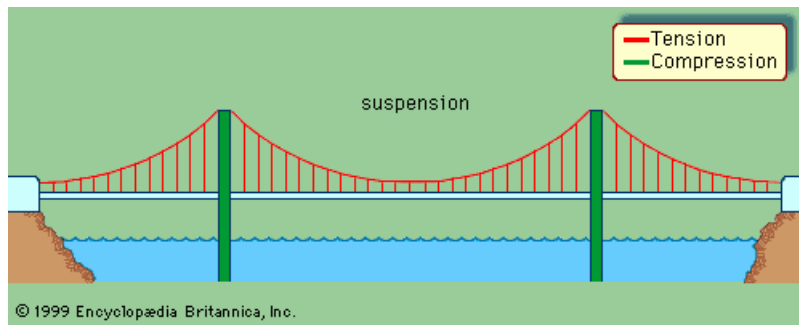


Figure 2.1. Members of a suspension bridge

1. Towers:

Towers are the members that support the cables and carry the loads on the bridge span to the foundation below. They are composed of columns or tower legs that are braced by struts or cross-girders to provide lateral stability to the structure. The portal and sway bracing are also necessary to brace the tower columns against buckling, to take care of lateral components from cradled cables and to carry wind stresses down to the foundation.

Tower legs are generally tapered at the top to meet the architectural requirements and also to provide resistance to the transverse forces. Tower legs are designed as columns to withstand the vertical reaction of the cables and as cantilevers to resist the unbalanced horizontal tensions. The latter will depend upon the saddle design (fixed or movable), the temperature and loading conditions.



Figure 2.2 Tower of suspension bridge (Golden Gate Bridge, SF)

Figure 2.2 shows different components of Golden Gate Bridge. Materials that are usually used for the construction of towers are either masonry or more commonly steel. Timber is also used occasionally. The application of steel to the suspension towers offers many advantages like lower costs and also the thermal expansion of steel towers balances with that of suspenders. Steel towers are made up of plates and angles to form either open or closed sections. If timber is used, each cable support consists of four battered posts with framed bracing, the two legs thus formed being connected at the top with cross-bracing.

2. Cables and Suspenders:

Cables are the only member that requires special care and knowledge for their erection. Cables are generally continuous over the saddles on top of the tower. They usually support and carry the loads from the hangers and transfer them to the towers. Whereas suspenders support the main truss and floor truss systems. The attachment of suspenders to the cable is generally made by means of cast steel collars called cable bands.

Cables are generally made of galvanized steel wires having an ultimate strength of 215 to 230 kips per square inch, and an elastic limit as high as 144 kips per square inch. Whereas the suspenders are generally galvanized steel ropes. They are manufactured in a diameter ranging from 1 to 3 $\frac{1}{2}$ inches and having a tested ultimate strength given by $80,000 \times (\text{diameter})^2$.

The diameter D of a cable, composed of n wires of diameter d , is given by

$$D = K \sqrt{nd} \quad (2.1)$$

Here K is void constant. The value of K varies between 1.09 and 1.12, depending upon the compaction.

3. Vertical and Lateral stiffening:

Due to deformations and undulations under the effect of moving loads, unstiffened suspension bridge should not be used. Hence if no stiffening truss is used, then the distortions and oscillations of the cables may be limited by using a small sag-ratio, by making the floor deep and continuous or by employing a latticed railing as a stiffening construction. Whereas, to give the structure resistance against wind forces, the most effective means is a complete system of lateral bracing.

The stiffening trusses are generally made from structural steel, but silicon steel or other alloy of steels may be used and for minor trusses even timber trusses have also been used.

Practically all modern suspension bridges are stiffened by means of a truss connection, either separate or incorporated in the cable system. The method adopted for providing vertical stiffness is by introducing diagonal stays between towers and the roadway. A different method consist of diagonal stays running from the tops of towers and meeting at a number of points along the span, so as to provide a triangular suspension for each point.

If the lateral bracing system is in the plane of the top and bottom chords of the stiffening truss, these chords may act as members of the lateral systems, otherwise separate wind chords must be provided. Another device that is used for securing the lateral stiffness is by building the cables and suspenders in inclined planes. But this system, however, does not appreciably increase the lateral stability of the structure. The main advantage of cradled cables is that they will help in bringing the resulting oscillations more quickly to rest.

2.3. Economic proportions for suspension bridges

The general ratio of side spans to the main span is about $\frac{1}{4}$ for the straight backstays, whereas for suspended side spans it is taken as $\frac{1}{2}$. Shorter ratios tend to increase the stresses or sections in the backstays than in the main cables. The length of the side spans is also governed by the existing shore conditions, such as relative elevations and suitable anchorages sites.

The economic ratio of sag to span of the cable between towers is about $1/9$ if the backstays are straight whereas it is taken as $1/8$ if the side spans are straight. For light highway and foot-bridges, these ratios may be revised as $1/10$ and $1/12$.

For efficient lateral bracing the width, center to center of outer stiffening trusses or wind chords should preferably not be less than $1/30$ of the span.

The proper depth of stiffening truss is determined by the degree of rigidity desired. Reducing the depth diminishes the cost. For highway bridges, the ratio of depth to the span may be made as low as $1/50$ to $1/70$. The increasing ratio of dead load to live load reduces the need for extraneous stiffening.

The economic utilization of the materials of construction demands that the predominating stresses in any structure should be those for which the material is best adapted. The superior economy of the suspension type for the long span bridges is due fundamentally to the following causes

- The very direct stress-paths from the points of loading to the point of support.
- The predominance of tensile stresses.
- The highly increased ultimate resistance of steel in the form of cable wire.

For heavy railway bridges, the suspension bridges will be more economical than any other type for spans exceeding about 1500 feet. As the live load becomes lighter in proportion to the dead load, the suspension bridge becomes more and more economical in comparison with other type.

Other than the economical consideration, the suspension bridge has many other advantages like light, atheistic, graceful, it provides a roadway at low elevation and also has a centre of low wind pressure, it can be easily constructed, materials used can be

easily transported, there is no danger during the construction phase and after construction, it is considered as the safest bridge.

2.4. Theories of Suspension Bridges

2.4.1 Rankine's Theory:-

A bridge comprising a roadway slung from suspension cables and stiffened in some measure by longitudinal girders at the road level was published by Rankine in 1858.

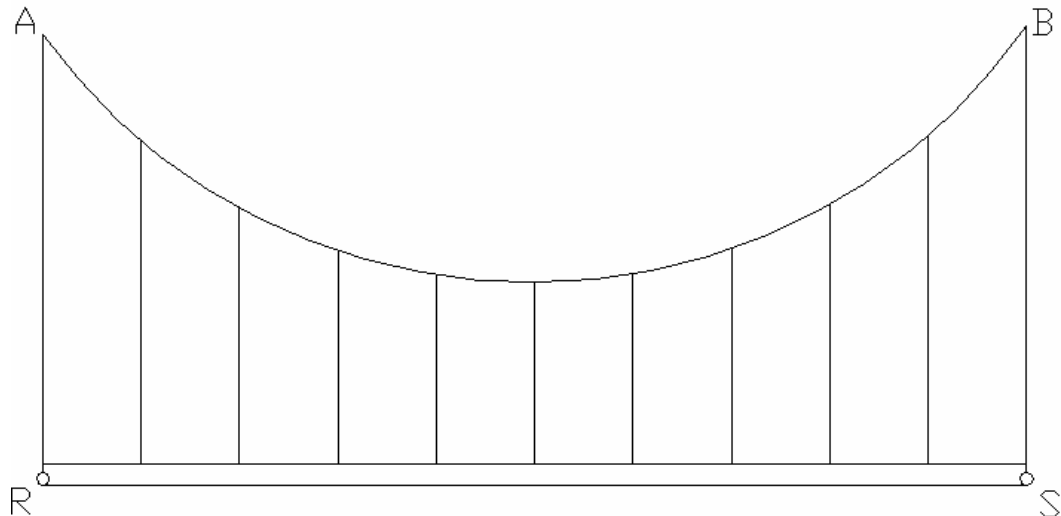


Figure 2.3. Stiffening girder supported by a cable through hangers

Considering a case wherein a stiffening girder (RS) is pinned at each end which is then suspended between two points A and B . Points A , B , R , S are assumed to be fixed in space. The cable and girder are also connected by numerous vertical suspenders figure 2.3. The basic assumptions of Rankine method are:

- Under the total dead loading on the bridge the cable is parabolic and the stiffening girder is unstressed.

- Any live loading applied to the girder is so distributed by it to the cable that the latter is called upon to carry a uniformly distributed loading across its whole span.

As a result of this assumption, the cable will retain its parabolic shape without any deformations. Hence the girder (*RS*), when subjected to a given system of live loads, will be in equilibrium under the following forces

- (a) The live loads acting vertically downwards.
- (b) Vertical reactions VR and VS at the pins *R* and *S*, acting either vertically upwards or downwards.
- (c) A uniformly distributed upward pull from the cables via the suspension rods, acting all along the girder from *R* and *S*, of intensity q per unit length.

There are three unknowns VR , VS and q and only two equations of equilibrium (vertical forces and moments) exist for their deformation. Rankine therefore made one more assumption. The value of q is equal to the total live load divided by the span L .

The assumed value of q can be found out directly whereas the remaining unknowns, VR and VS , can be found out from the two equations of equilibrium. Also, because of the third assumption, values of VR and VS are equal and opposite.

Hence, by this method, we can readily calculate the effects of a given system of live loads upon the tension in the cables, or the suspension rod loads, or the bending actions on the stiffening girder. But Rankine's theory was devoid of ensuring equilibrium without making any attempt to check that the displacements involved are compatible. For more understanding for this theory a case of two-pinned girder with a single concentrated load is discussed.

2.4.1.1. The Two-pinned Girder with a Single Concentrated Load:

Consider the effects of applying at Q in Figure 2.4, a single load P to the stiffening girder at a distance x from the end R . Then by the Rankine assumption, the uniform loading q between the girder and cable is given by,

$$q = \frac{P}{L} \quad (2.2)$$

From the condition of equilibrium for the girder, with this value of q ,

$$V_R = \frac{P}{L} \left(\frac{L}{2} - x \right) = -V_s \quad (2.3)$$

The bending moment diagram for the girder is thus given, as in Figure 2.4, by the difference between the parabolic curve, with a maximum ordinate of $qL^2/8 = PL/8$, and the triangular diagram, with a maximum ordinate of $\frac{Px(l-x)}{l}$. The peak value of the bending moment under the load is

$$M_Q = -\frac{Px(L-x)}{2L} \quad (2.4a)$$

When Q , the point of application of P , is at the center of the span, $x = \frac{l}{2}$ and

$$M_Q = -\frac{PL}{8} \quad (2.4b)$$

The variation of shear force on the girder, corresponding to the bending moment diagram is also shown in Figure 2.4. The foregoing actions on the stiffening girder are accompanied by an increase of tension in the cable due to a uniform pull downwards of q per unit span. The uniform loading produces an increased tension measured by its horizontal component h , of amount

$$h = \frac{qL^2}{8d} = \frac{PL}{8d} \quad (2.5)$$

Here d is the dip of the cable. This increase h is, by assumption, independent of the location Q along the span.

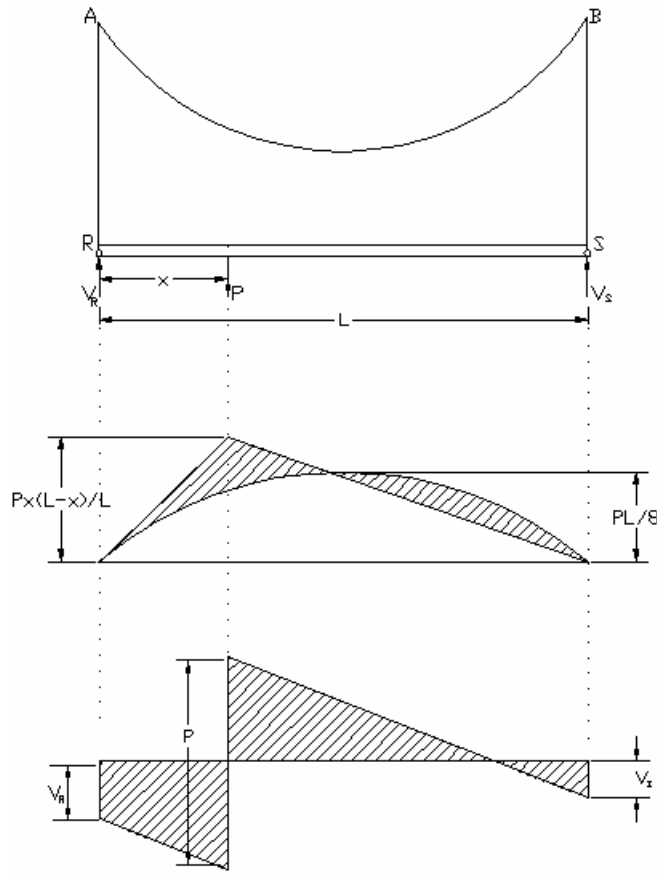


Figure 2.4.Shear and Bending Moment Diagrams for a single concentrated load

On the basis of this theory, Figure 2.5 gives the influence lines for bending moment and shear force in the stiffening girder at a section distance nL from the end R due to unit rolling load. It will be seen that as soon as the load enters on the span, the bending moment at the given section Z becomes,

$$M_Z = +\frac{1}{2} L(1-n)n \quad (2.6)$$

Thereafter the moment falls until the load reaches Z , when its value is

$$M_Z = -\frac{1}{2} L(1-n)n \quad (2.7)$$

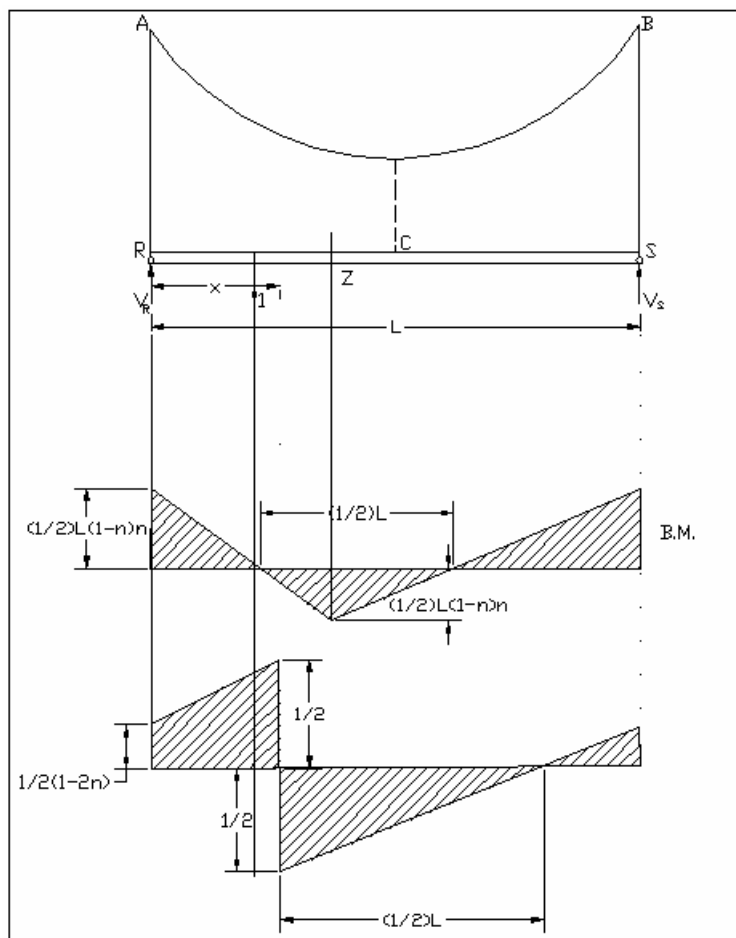


Figure 2.5.Influence lines for bending moment and shear forces in the stiffening girder

Further movement of the load reduces this negative moment till the value reaches that given by the equation (2.6), when the load is about to leave the span S. Thus the greatest bending moment arising during the passage of the load is that given by the above two formulas. When Z is at the center of the span C the greatest moment is

$$M_C = -\frac{1}{8}L \quad (2.8)$$

This agrees with equation (2.4). It is also clear from the influence line for shear force that, at any section Z , independent of value of n , the maximum shear force is $\pm \frac{1}{2}$ and rises when the unit load is at the section itself.

2.4.2 The Elastic Theory:

The basic assumptions of this elastic theory, when compared with the Rankine theory, are the same except for the 3rd assumption, which is related to the value of q

- q depends, in magnitude (still with uniform distribution), upon the elastic stiffness of the cable in tension and the stiffening girder in bending (and also to a lesser extent on the stiffness of the tower, etc.). In other words, the cable is treated as an inverted elastic parabolic arch, under uniform loading with a suspended elastic beam.

But, this treatment is essentially based on Hooke's Law, which doesn't support the non-linear behavior of a cable under heavy loads. However, for small deflections, the assumption of linear approach is justified and greater errors arise because q is assumed to be constant across the whole span, irrespective of the applied loading.

Thus, the elastic theory represents an advance over the Rankine Theory only in assessment of the magnitude of q , which is proved to be useful in practice.

2.4.2.1 Temperature Effects:

The cable is fixed at A and B , and so any increase in temperature would result in an increase in cable dip to accommodate the increase in its length. The stiffening girder, on the other end is simply supported and hence it will expand or contract to meet the effects of the temperature changes. Hence, if we consider a cable and a girder carrying dead load only, the effect of an increase of temperature will be to reduce the tensions in the

suspension rods and thus will introduce bending moments in the girder corresponding to sagging displacements between R and S .

The extension of the cable due to an increase of temperature t will be

$$\Delta l = \alpha t l \quad (2.9)$$

Here α is the coefficient of thermal expansion for the cable and l is its length. Also, the increase in dip at the centre of the span is

$$\Delta d = \frac{3}{16} \alpha t \frac{l^2}{d} \quad (2.10)$$

If it is assumed that the suspension rods do not extend appreciably, due either to changes of load or temperature, then this deflection Δd will be accompanied by a displacement of the girder by the same amount. On the assumption that the uniform loading carried by the suspension rods remains uniform, then the change in its loading q' must be such that

$$\Delta d = \frac{5}{384} \frac{q' L^4}{EI} \quad (2.11)$$

$$q' = \frac{384}{5} \frac{EI}{L^4} \Delta d \quad (2.12)$$

Hence,

And the change in H is

$$h' = -\frac{48}{5} \frac{EI}{dL^2} \Delta d \quad (2.13)$$

Using equation (2.10), the above results may be written as;

$$q' = \frac{72}{5} \alpha t \frac{EI l^2}{dL^4}$$

$$h' = -\frac{9}{5} \alpha t \frac{EI l^2}{d^2 l^2} \quad (2.14)$$

And the corresponding bending moments in the girder are

$$M = h' y \quad (2.15)$$

At the center the bending moment is

$$M_c = -\frac{9}{5} \alpha t \frac{EI l}{dL^2} \quad (2.16)$$

Now as per our assumption, since l is small as compared to L ,

$$M_c = -\frac{9}{5} \alpha t \frac{EI}{d} \quad (2.17)$$

2.4.3 Deflection Theory

This is a more advanced theory which is presented in terms of differential equations of the cable and stiffening girder by Melan. The focus was in the determination of increment h in the horizontal component of the cable tension due to some live loading p per unit length of the girder.

To understand this, consider a case of a single span bridge with the bending moment M on any section of the stiffening girder as

$$M = \mu + hy \quad (2.18)$$

Here μ is the bending moment, due to applied load, on the girder treated as isolated and simply supported at its ends. But, in deriving the above equation, it was assumed that the deflection v of the girder was negligible compared with the ordinates y of the initial cable shape. If this is not the case, then the allowance should be made for the corresponding increase v of the ordinate y . The bending moment has two terms, one of which, w , is due to dead load and the other, q , is due to live load. The moment term Hy due to w will be exactly balanced by μ_1 , due to dead loading, so that the initial moment M_1 on the girder is zero. Hence for the dead loading

$$M_1 = \mu_1 + Hy = 0 \quad (2.19)$$

Now, when the live loading is added, if we neglect v , the above expression becomes;

$$M = \mu_l + \mu + (H + h)y \quad (2.20)$$

$$= \mu + hy \quad (2.21)$$

If however, v is comparable with y , then

$$M = \mu_l + \mu + (H + h)(y + v) \quad (2.22)$$

$$= \mu + hy + (H + h)v \quad (2.23)$$

2.4.3.1 Basic Equations:

Considering the initial shape of the stiffening girder as that of dead load condition, then the measure of deflection would be wholly due to the live loading p and the induced suspension rod loading q . assuming the ordinary theory of bending, the flexure of the girder is

$$EI \cdot \frac{d^4 v}{dx^4} = p - q \quad (2.24)$$

For the balance of the vertical forces on the typical element of cable,

$$d(T \sin \theta) + w' dx = 0 \quad (2.25)$$

Here w' is the loading on the cable. But since

$$\begin{aligned} T \sin \theta &= H \tan \theta \\ \frac{d}{dx}(T \sin \theta) &= H \cdot \frac{d}{dx}(\tan \theta) \\ \frac{d}{dx}(T \sin \theta) &= H \cdot \frac{d}{dx}\left(\frac{dy}{dx}\right) \\ \frac{d}{dx}(T \sin \theta) &= H \cdot \left(\frac{d^2 y}{dx^2}\right) \end{aligned}$$

Equation (2.25) becomes,

$$H \cdot \left(\frac{d^2 y}{dx^2}\right) = -w' \quad (2.26)$$

But, the loading w' on the cable is the loading $(w+q)$ provided by the suspension rods, and the ordinates y have, due to q , increased to $(H+h)$. Hence equation (2.26), when applied to cables, for live load condition,

$$(H+h) \frac{d^2}{dx^2} (y + v) = -w - q \quad (2.27)$$

The dead load condition is,

$$h \left(\frac{d^2 y}{dx^2} \right) = -w \quad (2.28)$$

Substituting from equations (2.28) in (2.27),

$$h \left(\frac{d^2 y}{dx^2} \right) + (H+h) \frac{d^2 v}{dx^2} = -q \quad (2.29)$$

Hence, equation (2.24) and equation (2.29) relating respectively to the girder and the cable in terms of unknowns h , v and q . Combining these equations to eliminate q ,

$$EI \cdot \frac{d^4 v}{dx^4} - (H+h) \frac{d^2 v}{dx^2} = p + h \frac{d^2 y}{dx^2} \quad (2.30)$$

The above equation, in terms of h and v , is the fundamental differential equation of the suspension bridge in its classical form. There are two unknowns and one equation. The other equation is obtained by governing the condition of the extension of the cable and its overall length.

The elastic extension of the cable due to applied loading is,

$$\Delta l = \frac{hl}{AE} \quad (2.31)$$

Change in the length of the cable under the influence of w loading is given by

$$\Delta l = \frac{w}{H} \int_0^L x dv \quad (2.32)$$

On integrating by parts, noting that v is zero at both the limits

$$\Delta l = -\frac{w}{H} \int_0^L v dx \quad (2.33)$$

Combining equation (2.31) and equation (2.33) for the fixed ends of the cables;

$$\Delta l = \frac{hl}{AE} - \frac{w}{H} \int_0^L v dx = 0 \quad (2.34)$$

In many cases, the elastic extension of the cable is negligible and the above condition reduces to

$$\int_0^L v dx = 0 \quad (2.35)$$

Hence the problem of the suspension bridge, cast in these terms, thus reduces to the simultaneous solution of (2.30) and (2.34) or (2.35).

2.4.4 The Linearised Deflection Theory

In 1894, Godard proposed a linearization of the theory both for the simplification and for the advantages of the non-linear character deflection theory that it gave by making legitimate the use of superposition and influence lines. Later this theory was revised by H. Bleich (1935) and F. Bleich (1950), wherein, they discussed the natural frequencies and modes of vibration of suspension bridges. He also drew attention, by an essential relationship between Rankine, Elastic, and Deflection theories as indicated in Figure (2.7).

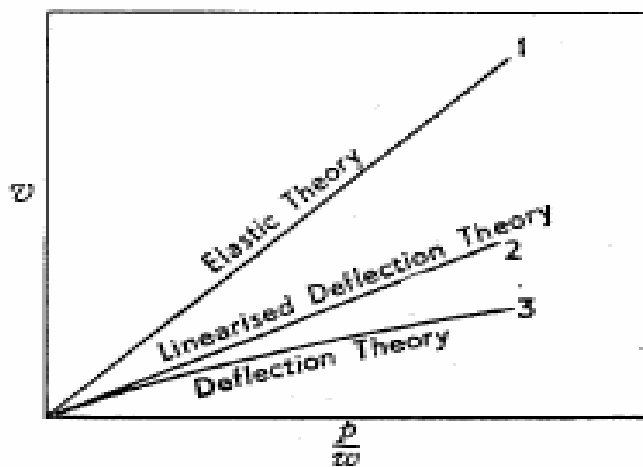


Figure 2.6.Comparison between different theories
(Pugsley, A.)

It is clear that, provided the live loading p is small as compared to the dead loading w , the deflection v will be proportional to p . It is also clear that as p increases compared to w , the bridge, due to the action of the cable, will become stiffer. These characteristics are illustrated by curve 3 (Figure 2.7). The linearized theory aims to produce straight line 2 tangential to the curve 3 at the origin. It is thus accurate for small values of p/w . For large values it's more accurate when compared with the elastic theory (curve 1). This is of particular relevance in long span bridges where the live loading is commonly small compared with the dead loading.

In the fundamental equation of deflection theory, the horizontal tension h due to p will be small compared with the initial tension H . Hence, neglecting h , the equation can be stated as,

$$EI \frac{d^4 v}{dx^4} - H \frac{d^2 v}{dx^2} = p + h \frac{d^2 y}{dx^2} \quad (2.36)$$

Hence, the basic equation becomes a linear differential equation with h directly proportional to p . As a result, v is also proportional to p , and the principle of superposition and the method of influence lines become applicable.

The second fundamental equation of deflection theory, relating to the extension of the cable still holds,

$$\Delta l = \frac{hl}{A_c E_c} - \frac{w}{H} \int_0^L v dx = 0 \quad (2.37)$$

The linearized theory proceeds by the simultaneous solution of above two equations, (2.36) and (2.37).

There are number of ways in which the above theory can now be developed. They are:

1. Tie Analog Method
2. Energy Method
3. Flexibility Co-efficient Method

3. DEAD LOAD, LIVE LOAD & BLAST LOADS

3.1 Dead load

The dead load includes the weight of all components of the structure, appurtenances and utilities attached, earth cover, wearing surface, future overlays and planned widening.

The model suspension bridge is a huge complex structure. The bridge deck, stringers, diaphragm and the connections are not modeled for simplicity. But to consider the effect of the all the non-modeled components, their weight is applied on the corresponding element. For instance, all the top chord members are subjected to a superimposed load of $0.508 \text{ k}/\text{ft}^2$, which may vary depending upon the type of diaphragm and the plate used for connection. Hence each and every member in addition to the self-weight is also subjected to a superimposed load which varies depending on the connections.

3.2 Vehicular Live Load

Generally the number of design lanes should be determined by taking integer part of ratio $w/12$, where w is clear roadway width in feet. In cases, where the traffic lanes are less than 12 ft, the number of design lanes should be equal to the number of traffic lanes, and the width of the design lanes should be equal to the width of the traffic lanes.

The extreme live load force effect shall be determined by considering each possible combination of number of loaded lanes multiplied by a corresponding multiple factor to account for the probability of simultaneous lane occupancy.

The multiplier presence factor should be included in various equations of distribution factors for both single and multiple lanes loaded. AASHTO HS-20 truck loading was used for the live load analysis on the bridge considering three traffic lanes.

3.3 Blast Load

Blast loads are considered as most extremes loads and even a small amount of blast can produce a serious damage to the structure. The blast waves produced on explosion travel even faster than the speed of sound. Blast pressure can create loads on structure that are many times greater than the normal design loads and blast winds can be much more severe than hurricanes.

Blast waves are produced whenever an explosion takes place. These waves propagate in the form of spherical waves resulting discontinuities in the structures. Some of these waves transfer across the structures while remaining are reflected back. During this wave propagation, high pressure and high temperature are generated which travel across the least resistance path of the structure. This entire process of the wave generation and propagation last for a few milliseconds.

The initial step in blast design or analysis is the determination of the blast loads. The factors that consider attention are energy absorption, load combinations, critical elements, and structural redundancy to prevent progressive collapse of the structure.

If an explosion occurs on the top of the bridge, bridge deck will experience the downward thrust of the overpressure, which will be transmitted to the hangers, to cables and towers. Foundation will experience blast-induced vertical and overturning forces. If the blast load is applied at the bottom of the bridge, deck slab and the supporting girders will experience an upward pressure for which they are generally not designed. Structurally these components are only designed to carry vertical downward forces. So, when they are subjected to vertical upward forces, the bottoms of the deck member are subjected to compression and top is subjected to tension, for which they are not normally designed for. Towers and foundations are also subjected to vertically upwards and lateral forces and also overturning moments. Failure of the system is obvious unless otherwise they are designed for the vertical upward forces.

3.3.1 Equivalent Static Loads

The method to determine the equivalent static load is a complex phenomenon as the blast load diminishes with the distance from the point of explosion. In the TM 5-1300 Manual, Structures to Resist the Effects of Accidental Explosions, developed by the US Department of Defense in December 1990, an empirical formula equation (3.1) was used to find the scaled distance. The amount of blast pressure generated is inversely proportional to the scaled distance, which is presented in the chart in the TM 5-1300 Manual. The empirical formula to find the scaled distance, Z (ft), is

$$Z = \frac{R}{(W)^{\left(\frac{1}{3}\right)}} \quad (3.1)$$

R is the distance of target from point of explosion (ft) and W is the equivalent TNT weight of charge (lbs).

Using this formula and the chart in TM 5-1300, a computer program named ATBlast was developed which calculates the blast loads for known values of charge weights and the standoff distances. The conversion to the blast load for the 500 lb of TNT with a minimum and maximum range of 4 ft and 25 ft at 1 ft increment is converted into equivalent static load using ATBlast is presented in the Table 3.1 where R represents the distance of target from the point of explosion and W is the equivalent TNT weight of charge, V is the shock front velocity, TOA is the time or arrival, P is the pressure, I is the impulse whereas td is the duration. These resulting static loads were applied at different locations on the modeled bridge.

R <i>(ft)</i>	V <i>(ft/sec)</i>	TOA <i>(msec)</i>	P <i>(psi)</i>	I <i>(psi-msec)</i>	td <i>(msec)</i>
4	13.13	0.22	2511	9312	0.68
5	13.39	0.3	1884	6336	0.66
6	10.11	0.4	1480	4577	0.66
7	9.13	0.5	1198	3645	0.67
8	8.34	0.61	991	2953	0.68
9	7.69	0.73	832	2462	0.7
10	7.13	0.87	707	2098	0.73
11	6.63	1.01	607	1820	0.76
12	6.2	1.17	524	1602	0.8
13	5.81	1.34	456	1426	0.84
14	5.45	1.52	399	1283	0.89
15	5.14	1.71	351	163	0.95
16	4.85	1.91	310	1063	1.01
17	4.58	2.13	275	977	1.08
18	4.34	2.35	245	903	1.15
19	4.12	2.59	219	839	1.23
20	3.92	2.84	197	783	1.32
21	3.74	3.11	177	733	1.41
22	3.57	3.38	161	689	1.51
23	3.42	3.67	416	650	1.61
24	3.28	3.97	133	615	1.72
25	3.15	4.29	121	583	1.84

Table 3.1: Equivalent Static Parameters for 500 lb of TNT Explosion

The variation of the pressure with respect to distance from the point of explosion is shown in Figure 3.1. The closer is the explosion to structure; the more severe is the resulting pressure and the likelihood of structural damage.

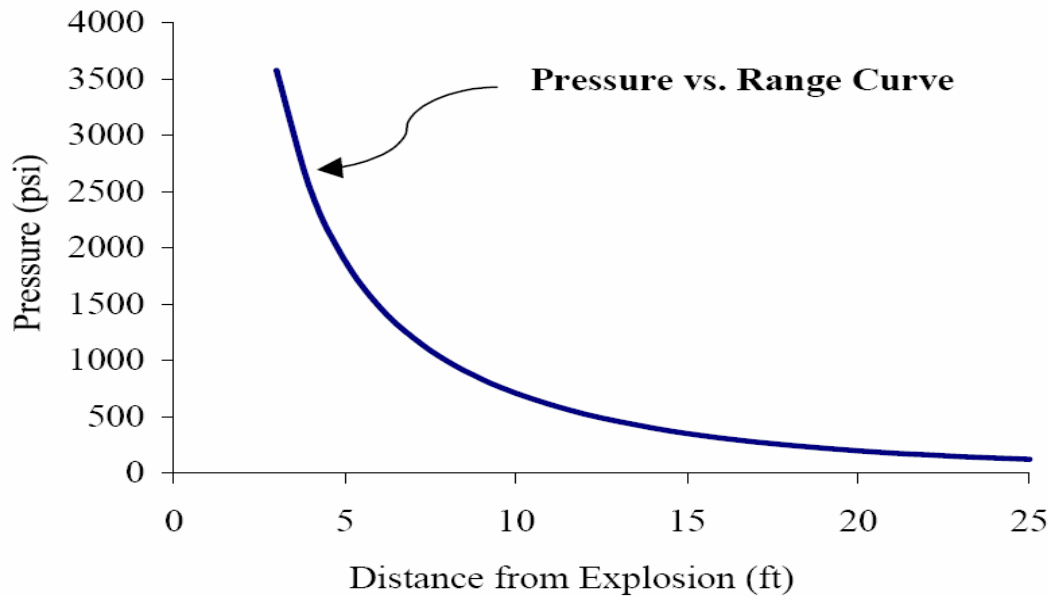


Figure 3.1 Variation of pressure from distance of explosion
 (Anwarul Islam, 2005)

Figures 3.2 and 3.3 show elevation and plan views of typical blast pressure distribution on a bridge surface. In order to simplify the method of blast distribution, distribution of blast load was carried out as shown in Figure 3.3.

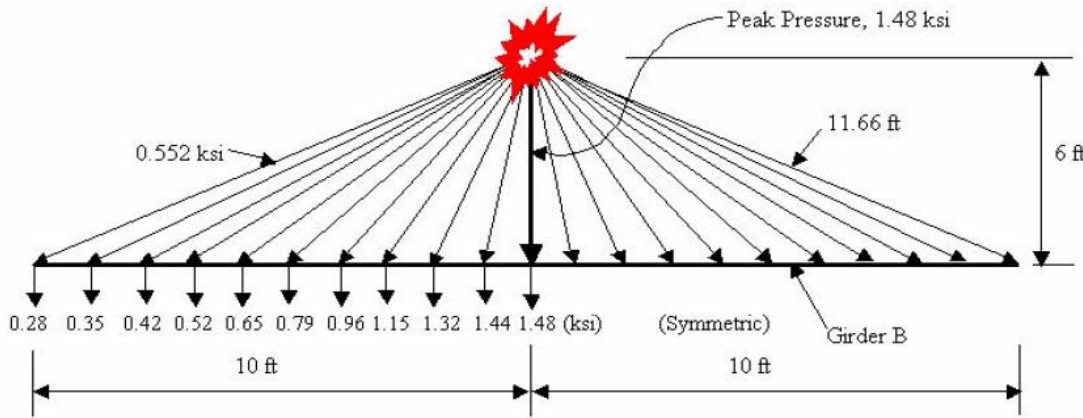
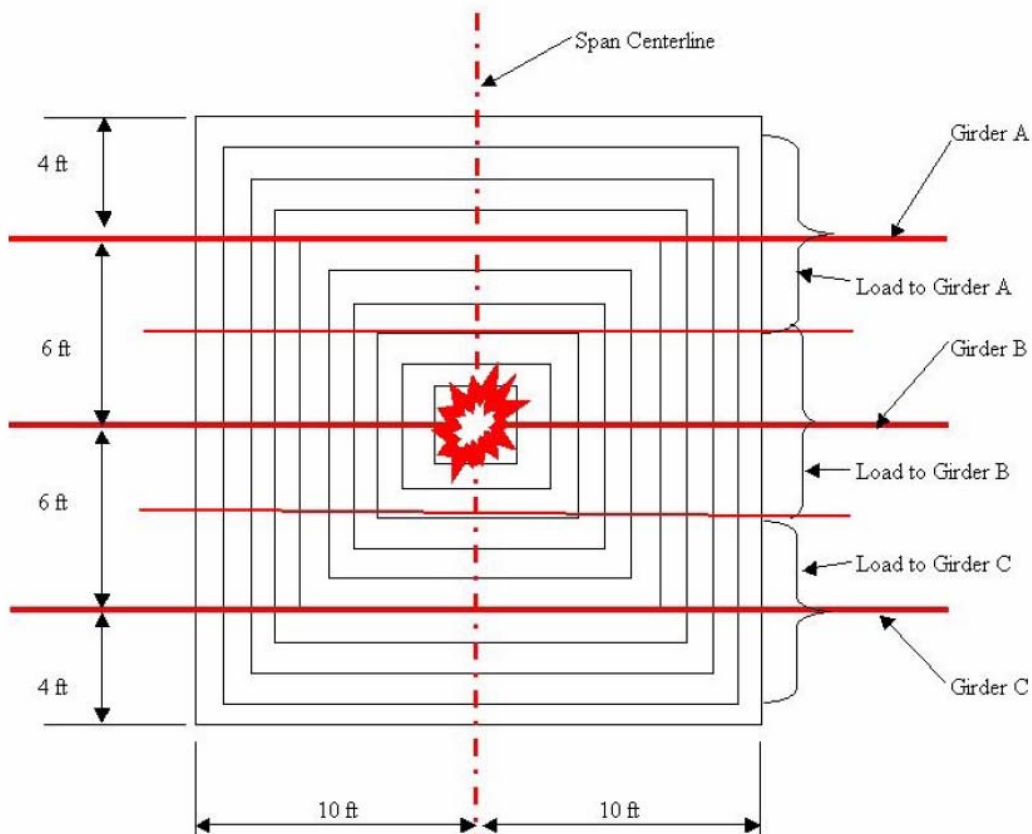


Figure 3.2 Blast pressure distribution on bridge deck (elevation)
 (Anwarul Islam, 2005)

In this case, the highest load is 1.48 ksi generated due to an explosion of 500 lbs of TNT at a height of 6 feet from the bridge deck. Girder B with a length of 20 feet experiences the highest average pressure of 0.77 ksi for a length of 20 feet, which is approximately 50% of peak value of 1.48 ksi. The adjacent girders A and C experience a load of 0.5 ksi which is again equal to 30% of the peak value of 1.48 ksi. This distribution of blast pressure is commonly known as 50 percent distribution rule and 30 percent distribution rule respectively.



Average pressure directly on Girder B = 50% of 1.48 ksi = 0.74 ksi

Average pressure on Girder A or C = 30% of 1.48 ksi = 0.44 ksi

Figure 3.3 Blast pressure distributions on bridge deck (plan)
(Anwarul Islam, 2005)

Similarly, by following this average distribution rule, blast pressure can be applied on the critical members of the bridge structure for different blast load cases. If the blast

explosion was to occur at a distance of 4 feet from one of the towers, approximately 2.5 ksi of highest blast pressure will be produced (Table 3.1). Out of which about 1.25 ksi, which is 50% of the 2.5 ksi, would act on column. At the same time, the girder bottom at a distance of 13 feet would experience approximately 0.23 ksi (50 percent of 0.46 ksi) pressure and slab bottom at a distance of 17 feet would take an average pressure of 0.08 ksi (30 percent of 0.275 ksi). On the other hand, if the explosion had occurred on top of the bridge, part of the deck at 6 feet below the point of explosion would experience around 0.74 (50 percent of 1.48 ksi) and 0.45 ksi (30 percent of 1.48 ksi) pressure through the beam which is closest to explosion and its adjacent beams respectively. Depending on the amount and type of damage which the bridge components would suffer, the bridge would be classified into partially or completely out of service.

3.3.2 Comparison of Blast loads and Seismic Loading:

Both of these loads are dynamic loads and they produce dynamic structural response. The focus of these loads on the structural response is on life safety rather than preventing structural damage. Hence while dealing with these loads, the designs are more performance based which includes life safety issues, progressive collapse mechanism, ductility of certain critical components, and redundancy of the whole structure.

Differences between these two types of loadings are presented in Figure 2.4 and also summarized in Table 3.2. Blast load damages the structure through the spherical propagating waves which directly hit the structure to destroy it, while earthquake waves damages the structures through lateral ground shaking and causes destruction through the ground movement. Hence blast load has direct effect on the structure while seismic waves don't act directly on the structure. Also blast load is more of local load and leaves its effect on a particular region while seismic load is a global load.

Blast load are of shorter duration compared to the seismic loads. Although both of these loads are highly unpredictable in nature, seismic activity can be categorized based on geographical locations.

Blast Loads	Seismic Loads
Damages structures through propagating spherical pressure waves.	Damages structures through lateral ground shaking.
Higher amplitude if explosion is targeted on a particular structure.	Not targeted on any particular structure.
Directly hit the structure.	Seismic epicenter develops few miles down from the ground surface.
Shorter duration in terms of milliseconds.	Longer durations in terms of milliseconds.
Highly unpredictable.	Highly unpredictable, but can be well defined in the aftermath of an earthquake.
More localized action.	More global action.
Does not depend on geographic locations.	Does depend on geographic locations.
Can be categorized by stand off distances and charge weight.	Can be categorized on geographical locations.
Can be prevented by implementing necessary security measures.	Cannot be prevented.

Table 3.2: Summary of Seismic loading and the Blast loading Differences

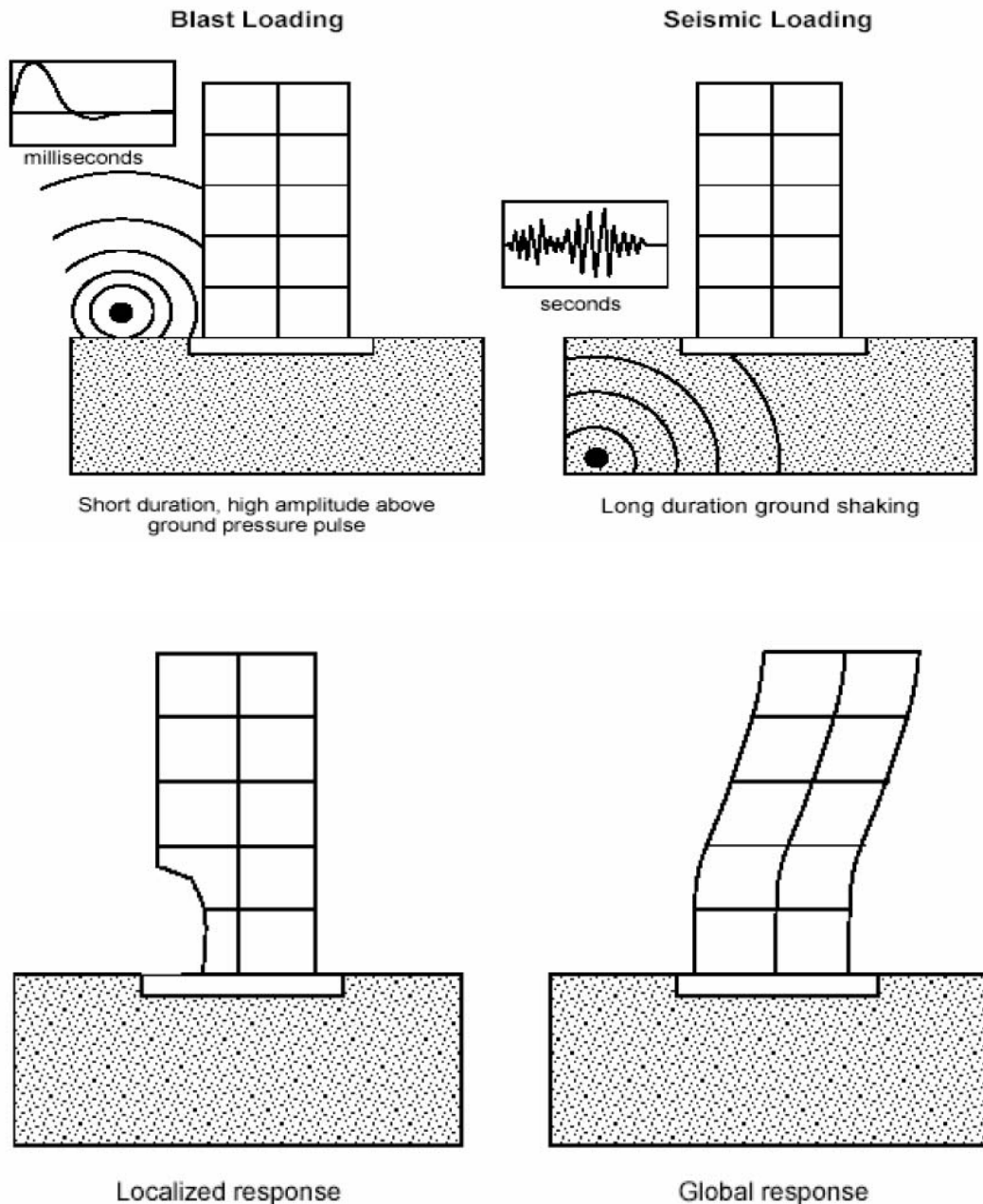


Figure 3.4 Comparison of blast and seismic actions on structures
 (NIST 2001)

While magnitude of blast cannot be predicted, seismic magnitude can be precisely described in the aftermath of an earthquake. Progressive collapse of structure is the most serious consequence of explosion. Also, there are very less codes and standards available

for the unpredicted blast loads, whereas many codes and standards give a better knowledge to make a building or structure resistant to the seismic loadings.

In summary, while the effect of blast loading is localized compared with an earthquake loading, the ability to sustain local damage without total collapse (structural integrity) is a key similarity between seismic-resistant and blast-resistant design (NIST 2001).

4. SUSPENSION BRIDGE IMPLEMENTATION

For carrying out the static and dynamic analysis of the bridge structure, Visual Bridge Design System (VBDS) and SAP2000 software were used. The author has presented a very brief summary which explains the capabilities of using this software.

4.1 VBDS

Visual Bridge Design System (VBDS) is new generational bridge analysis and design software based on years of experience of both bridge engineering practice and software development. Its design and development adopted entirely the state-of-art software development technology, such as relational database management, graphical user interface, visualization and object oriented graphical integration (object ARX).

The core of the system consist of VBDSKNL, the bridge Finite element analysis (FEA) Kernel, VBDSPRE, the preprocessor, VBDSPST, the postprocessor and VBDSTDN, the prestress tendon configuration. The outstanding feature of the system is to adopt the unified core database.

VBDSKNL is a specifically designed to meet the special requirements of the spatial structure analysis of a bridge built in multiple construction stages. Also all the analysis results can be visualized through graphs or tables in the foreground while the analysis is processed in the background. The main features includes 3D beam, truss and shell elements, analysis of multiple load cases, prestressing force calculations, dynamic modal analysis, elastic stability analysis, large deformations and other geometric non-linear analysis.

VBDSPRE creates the finite element modeling. AutoCAD is adopted as a platform for modeling. Special features includes auto-mesh for wire frames and surface models,

editing boundary conditions and multiple load cases and data exchange between finite element analysis systems.

VBDSPST is used to graphically present the bridge analysis results. Besides the basic functions for post-processor which are internal forces and displacement graphs and stress contours, it also includes special features like plotting for the influence lines and influence surfaces, plotting for live load envelope, AASHTO and user defined load combinations and graphical representation of the incrementing, accumulative and envelopes results.

VBDSTDN is to define cross section and prestress tendon profiles graphically and parametrically and to establish prestress tendon model together with bridge structure model. It also contains special features like importing the AutoCAD drawings, prestress loss calculations, geometrical property calculation of a cross section and defining the cross sections of a bridge via graphical or parametric methods.

Bridge FEA Kernel is specially designed and developed for the bridge structure engineers. The analytical functions of the Bridge FEA Kernel includes elastic linear analysis, dynamic modal analysis, elastic stability analysis, geometric nonlinear analysis with initial stress and strain considerations and also consideration of nonlinear sag effectiveness of long cables. It adopts a new automatic time incremental method for analysis of creep and shrinkage of concrete bridges. The live load includes all the loads specified in AASHTO LRFD Bridge Design Specifications and some other codes from different countries.

4.2 SAP2000 Software

This is a product by Computer and Structures INC. Founded in 1975 by company President and CEO, Ashraf Habibullah, is recognized worldwide as the innovative leader in the development of software tools for the analysis and design of structures. The other major products include STABS, SAFE, PERFORM 3D, CSI COL. These products from

the CSI are used by thousands of engineering firms involved in the design of buildings, bridges and other major projects in over 160 countries.

Since its introduction over 30 years ago, SAP2000 follows in a same tradition featuring a very sophisticated, intuitive and versatile user interface powered by an unmatched analysis engine and design tools for engineers working on transportation, industries, public works, sports and other facilities.

Bridge Designers can use SAP2000 Bridge templates for generating bridge models, automated bridge live load Analysis and design, bridge base isolation, bridge construction sequence analysis, large deformation cable supported bridge analysis and pushover analysis.

SAP2000 features a state-of-art user interface, visualization tools, powerful analysis and design engines with advanced finite element as well as dynamic capabilities. From model generation, analysis and design of steel, concrete, timber, aluminum, timber and many other materials can be analyzed in SAP2000.

SAP2000 has the capabilities of generating different elements with user defined degrees of freedom for each 3-nodes, 4-node, or even 8-node elements. Loads can be applied on the structure in the form of nodal loads, member loads, temperature loads, uniform pressure over the surface, trapezoidal loads and also surface expansion loads.

The whole modeling of the suspension part of the bay bridge was done on the SAP for carrying out the non-linear analysis for the blast load. The area loads were applied in the form of uniformly distributed loads on each of the members. The behavior of each of the element under the effect of blast was studied from the output generated by the SAP2000. The output of the software presents results including moments, shears and displacements. Moreover, moments and shears, at each node and at any point within the element, can be easily obtained from the software output.

All the above features make SAP2000 the unique and most appropriate software for the analysis and design of bridge structures.

4.3 Bridge Model

The modeled bridge is a typical suspension bridge with a center span of 1600 feet and side spans of 675 feet each. For the better understanding of the whole bridge, it is mainly divided and modeled into six different components, cables, hangers, floor beam truss, main truss, towers and lateral bracings.

1. Towers:

The Suspension bridge consists of two steel towers, each with two tower legs. The total length of each tower leg is 351'-0" and each tower leg is composed of 9 tiers. The towers are tapered at the top. The width of tower at base in transverse direction is 10'-0" which tapers to 8'-0" at the top. Whereas in longitudinal direction, the bottom width is 13'-0" which tapers to 9'-0" at top.

The lateral bracing is provided in the form of the struts. There are in all six struts, one top strut, four intermediate struts and one roadway strut. The cross section of the tower leg shows the use of end plates and longitudinal stiffeners. Also stainless steel shims are provided to obtain improved bearing between tower tiers.

Openings are provided in tower diaphragm for electrical conduits except in struts. Also stiffeners are provided in all the struts.

2. Cables and Suspenders:

The cable is based on use of galvanized wire of 0.204 inches in diameter, made into 37 strands of 91 wires each. Gross metallic area of cable is 110.14 square inches. Diameter of cables after compaction and before wrapping is about 13 ½ inches. Also,

if the average diameter of the wire is less than 0.204 inches, increase in the number of wires so as to secure the same total area of wires in the cables.

The suspender ropes shall be constructed of prestretched galvanized wire and shall be composed of six strands around an independent wire rope center. The nominal diameter of the rope is $1\frac{5}{8}$ inch. Suspender ropes are to be vertical under full deal load at normal temperature of $68^{\circ}F$. Hand ropes shall be single strand approximately 1 inch diameter.

3. Main Truss and Floor beam truss:

The total length of the main truss member is 2950 feet and a height of 16 feet. The total width of the floor beam truss is 49 feet. A light weight concrete deck is constructed on this bridge with a width of $6\frac{1}{2}$ inches which includes $\frac{1}{2}$ inch of monolithic wearing surface. The deck is supported on 9 stringers which are wide flange sections. The top and bottom chord members are a closed section made from 2-13x4 C shaped sections placed back to back at 13 inch and covered with top and bottom Stay plates.

4.3.1 VBDS Bridge Model

VBDS has a strong advantage of transferring the drawing from the AutoCAD. By making use of this advantage the initial drawing was done in AutoCAD. The drawing was done by just drawing lines which actually represented the elements of the structure. In this way, the complex bridge structure, if created in VBDS, was simplified by using AutoCAD.

The total number of nodes and elements that were used for creating this model are 2978 and 5264, respectively. These elements were further divided into sub groups, cables, hangers, towers, floor beam truss, main truss and lateral bracing.

Description of each of sub group with total number of elements used along with the total length of the each members and the type of the element used are listed down in Table 4.1

TYPE OF ELEMENT	TOTAL LENGTH	NUMBER OF ELEMENT	MEMBER TYPE
Towers	1466.32	260	Truss
Cables	6087.62	148	Truss
Hangers	9037.77	142	Truss
Floor Truss	30536.75	2046	Truss
Main Truss	23547.98	1710	Truss
Lateral Bracing	18140.95	868	Truss

Table 4.1 Description of different sub components of the bridge model

The material that was used in construction of the bridge was galvanized wire, wide flanges and other compound steel sections. The material property that was applied to the model bridge for actual represent of the structure is as shown in Table 4.2

MATERIAL	STEEL
Density	0.49 kips per cubic feet
Co-efficient of linear expansion	6.5E-6 / °C
Young's modulus	4176000 kip/ft ²
Poisson ratio	0.3

Table 4.2 Material property

The property was assigned to each of the line that was borrowed from the AutoCAD drawing. Thus the lines in AutoCAD are now transferred into elements which represent

the actual nature of the structure. The next step after assigning the correct sectional properties and the material properties was to apply the load on the structure.

For the sake of the simplicity, the diaphragm and connections were not modeled, but their corresponding weight was taken and applied on the particular members. For example, the deck slab and stringers were not designed, but the slab weight and the weight of stringers was calculated and distributed on top chords of the floor beam truss. Similarly the weight of connections was distributed on the bottom chords and corresponding wide flanges in the floor beam and main trusses.

VBDS automatically transfers this uniformly distributed load into corresponding joint loads and gives the shear, deflections and bending moments on each element. The entire bridge after modeling is shown in Figure 4.1.

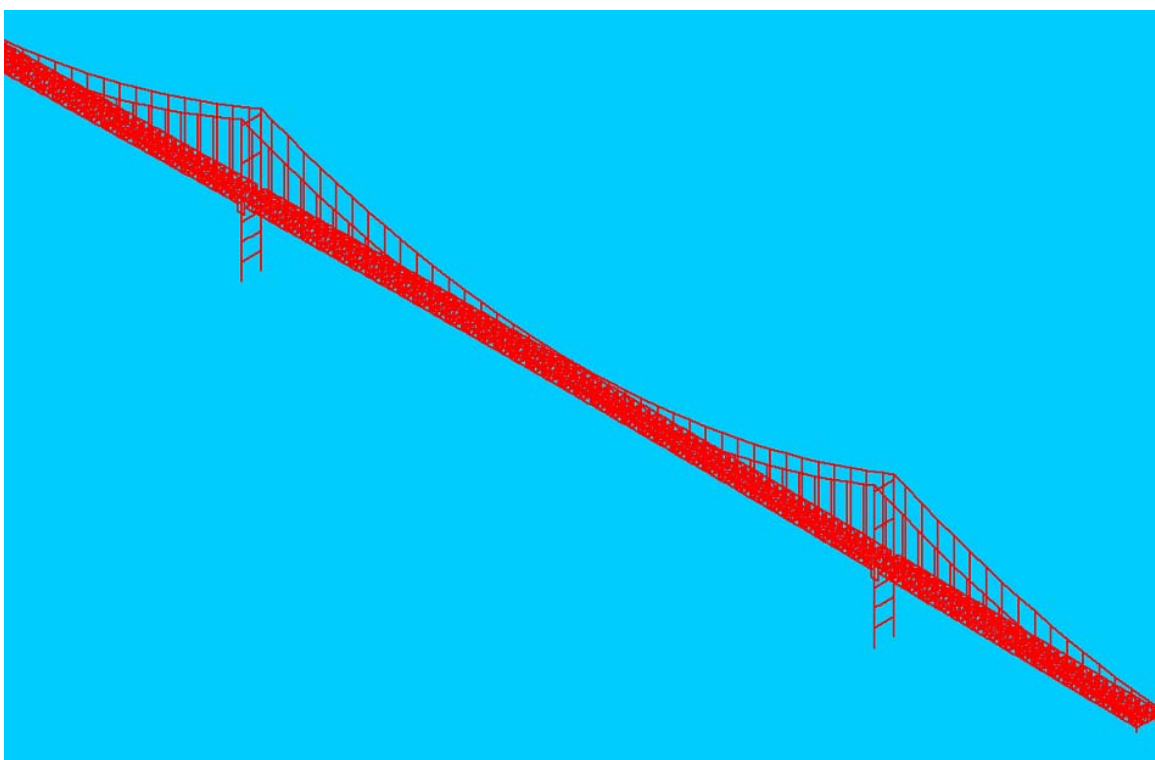


Figure 4.1 Bridge model in VBDS

The dead load was applied on the entire bridge and the analysis of the bridge was carried out. But for the live load, only the quarter of the bridge was modeled (Figure 4.2) and analysis was carried out.

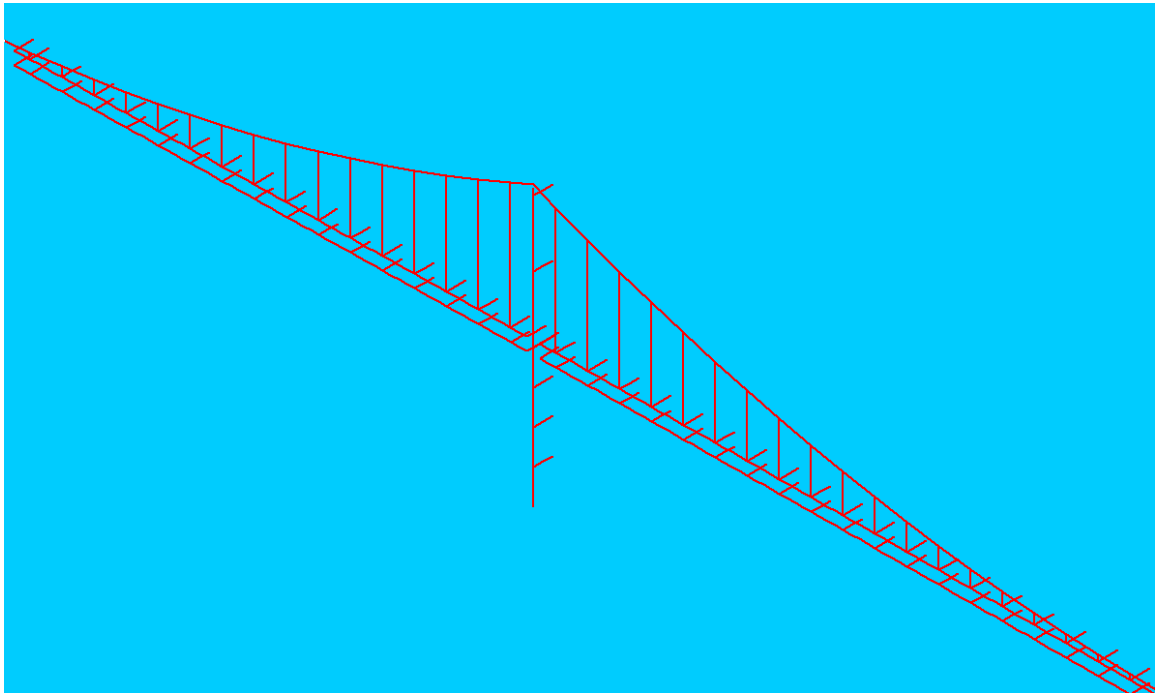


Figure 4.2 Live load analysis model in VBDS

4.3.2 SAP2000 Bridge Model

The model was transferred into SAP2000 for carrying out the blast analysis on the bridge model. The input file of the VBDS consisted of the node co-ordinates and the member incidences including material and element properties (Figure 4.3). However the application of loads on each member was not directly transferred from the VBDS model. The loading was divided into dead load, area load and blast loading. Three cases of blast loading were taking into consideration. The geometric stiffness enhancement of main cables is significant. An average initial axial force of 7,000 kips, which is due to dead load, was considered in the dead load and live load analyses. In the dead load analysis, such an initial axial force is obtained from a couple rounds of iteration.

As the elements and nodes were directly borrowed from the VBDS, the number of elements and nodes were the same in both these software. The non-linear analysis was carried out for this structure in SAP2000. The area loads were applied as uniformly distributed load on corresponding members. This uniformly distributed load was automatically transferred into joint load by the software.

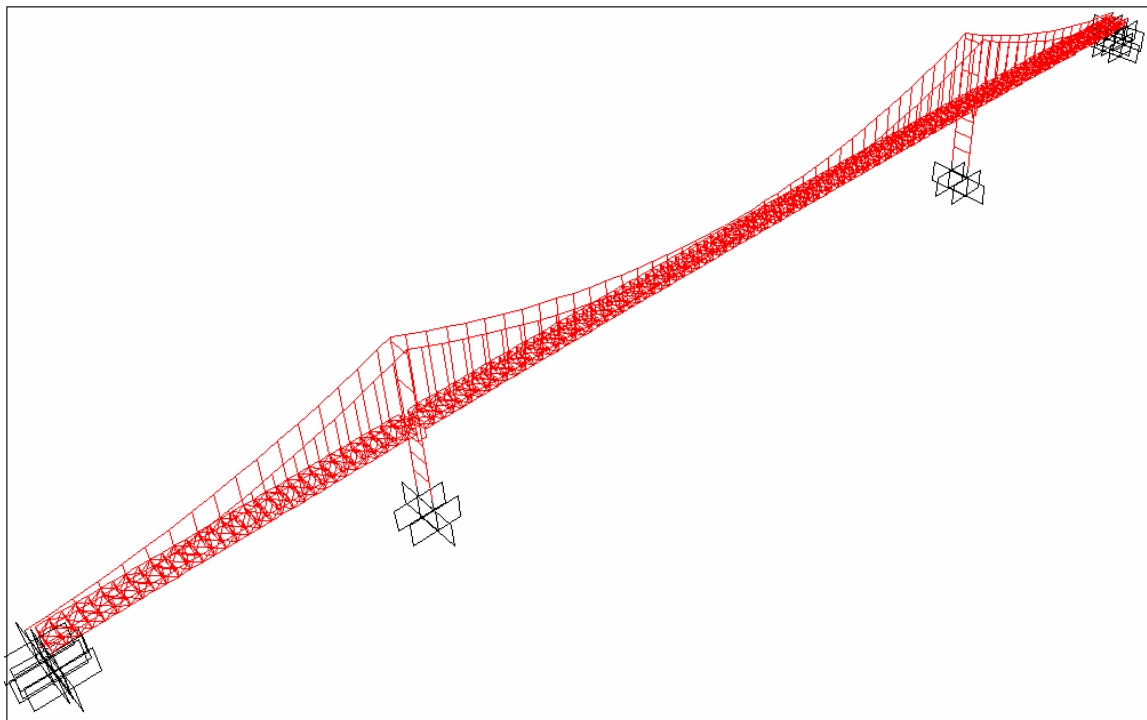


Figure 4.3.Bridge model in SAP2000

The only difference between the two software was the orientation of the members once they were modelled by sharing the nodal co-ordinates and the element lengths. The orientation of the member was assigned by producing the reference vectors, while in SAP2000; they were oriented along the minor axis of the members.

The analysis was carried out in SAP2000 with extraction of first 12 modal frequencies. The result was done for three blast load cases and the axial loads, shear forces and the bending moments on each of the critical members was studied.

5. BLAST LOAD CASES

The explosion loads (blast loads) were considered as an extreme event loads with a factor of 1.00 according to AASHTO LRFD Bridge Design Specification (AASHTO 2003). In addition to this the self weight of the structure was also considered and multiplied with a factor of 1.25. The equation which governs the extreme load with combination of dead and live load is as presented in Equation 5.1. The effect of truck live load is negligible compared to that of blast load and hence it is not considered in the analysis.

$$W_T = 1.25(D.L.) + 0.5(L.L.) + 1.00(E.V.) \quad (5.1)$$

Here, W_T = total load, $D.L.$ = dead load, $L.L.$ = truck live load and $E.V.$ = extreme event load.

Converted blast load were divided into three different groups based on their position of application on bridge model. This structure after application of blast loads cases was analyzed using software SAP2000. For ease of load applications, the blast loads were converted into point loads and applied at the specific critical locations on the bridge model. The various load cases, formed by these uniformly distributed loads of 500 lb of TNT, as by BRP, a 500 lb of TNT is the most extreme case and all the bridge normally fail at this load are presented in the following sections and summarized in Table 5.1.

Load case	location	Blast set-back
Case 1	Mid-span of the center span	6 feet above the deck
Case 2	Mid-span of the end span	6 feet above the deck
Case 3	End-span of the center span	6 feet above the deck

Table 5.1: Load Cases

5.1 Load Combination 1

As shown in Figure 5.1, this load combination was defined to take place at the mid-span of the center span at 6 feet above the deck. It was assumed that the effective area of 20 feet by 20 feet experiences a downward pressure, considering the 30-degree angle of projection. The three consecutive girders (stringers) that are spaced at 6.125 feet on center are affected by this blast load application. This pressure is distributed along the entire stringer by using 50 percent rule and 30 percent rule. Using the area tributary area and the distribution rule, the total pressure acting on the center stringer (the one above which the blast takes place) is subjected to a 0.74 ksi (50 percent of 1.44 ksi) and the two adjacent stringers to this girder are subjected to 0.44 ksi (30 percent of 1.44 ksi). These pressures are further converted into uniformly distributed load by multiplying each pressure with the tributary width of 6.125 feet. The values thus obtained are 653 kips per foot (On center stringer) and 388 kips per feet (adjacent stringers). These uniformly distributed loads were again converted into equivalent nodal loads. Finally, the nodal loads obtained are 6530 kips (center stringer) and 3880 kips (adjacent stringers).

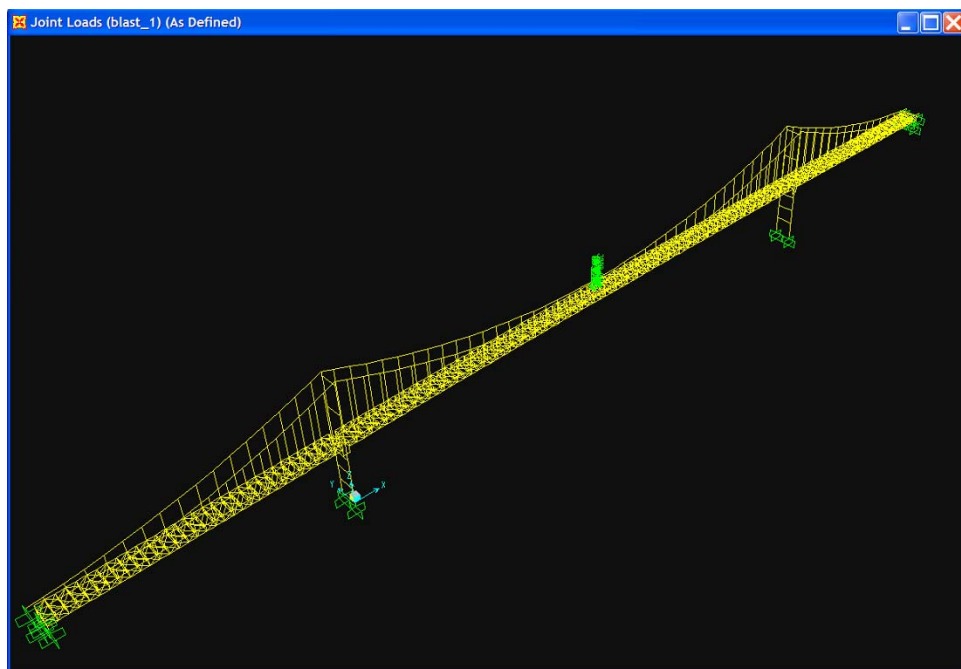


Figure 5.1: Application of Blast load at center of mid-span

The axial load and the moment produced by these loads are presented in Figure 5.2 and Figure 5.3 & 5.4 respectively. In Figures 5.2, 5.3 and 5.4, the axial force and bending moment represented by the yellow color and blue color are due to minimum and maximum envelope values.

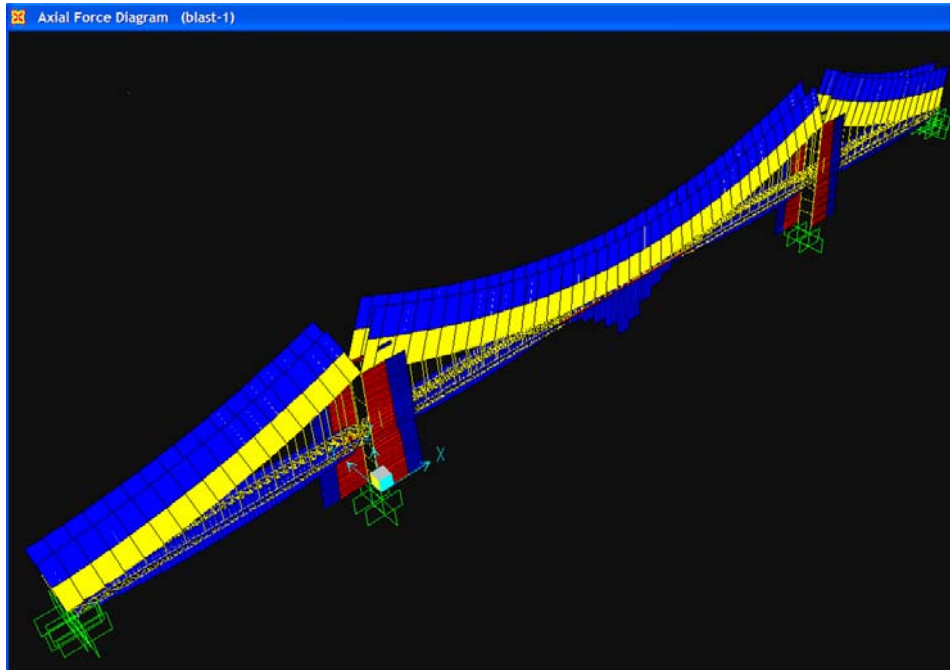


Figure 5.2: Axial force diagram for blast load case 1

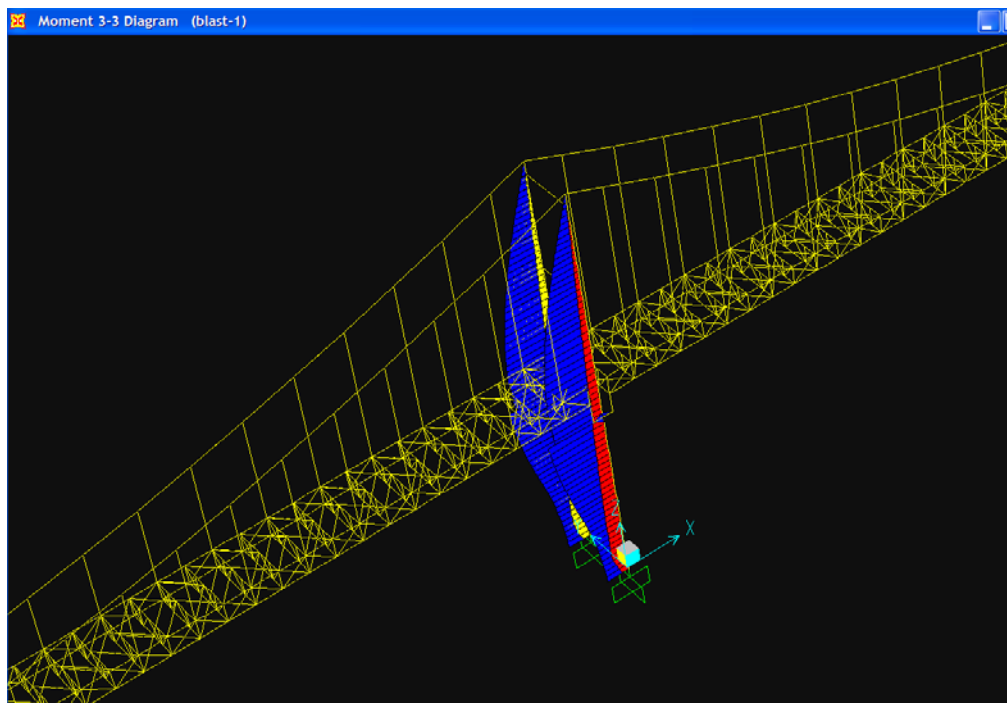


Figure 5.3: bending moment diagram on tower for blast load case 1

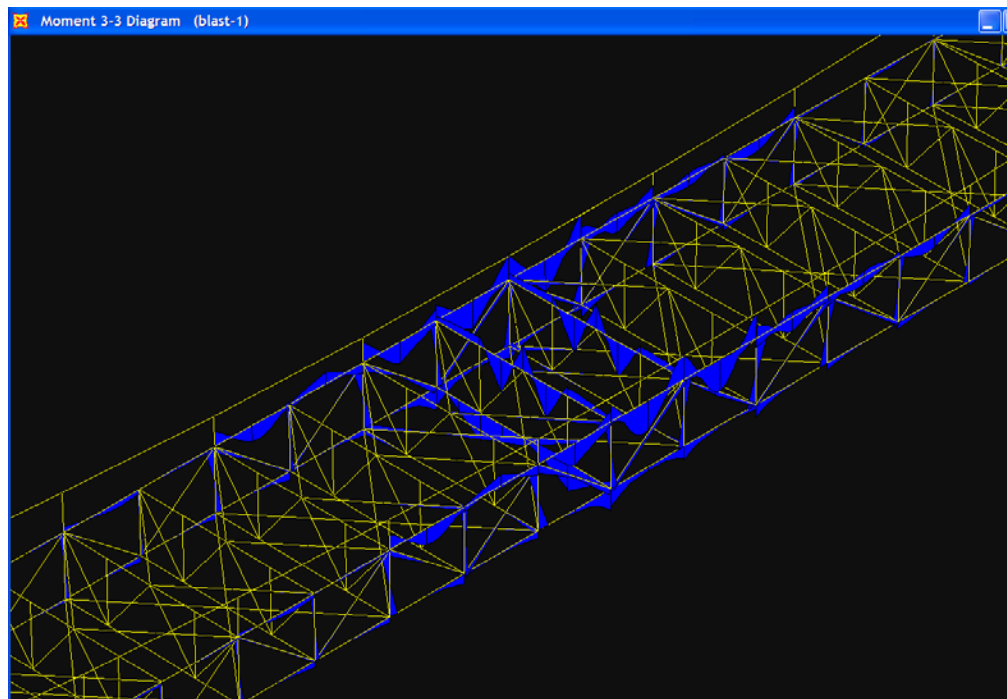


Figure 5.4: bending moment diagram at the location of blast load case 1

5.2 Load Combination 2

As shown in Figure 5.5, this load combination was defined to take place at the mid-span of the end span at 6 feet above the deck. Similar to load combination 1, it was assumed that the effective area of 20 feet by 20 feet experiences a downward pressure, considering the 30-degree angle of projection. The three consecutive girders (stringers) that are spaced at 6.125 feet on center are affected by this blast load application. This pressure is distributed along the entire stringer by using 50 percent rule and 30 percent rule. Again similar to load combination 1, using the area tributary area and the distribution rule, the total pressure acting on the center stringer (the one above which the blast takes place) is subjected to a 0.74 ksi and the two adjacent stringers to this girder are subjected to 0.44 ksi. These pressures are further converted into uniformly distributed load by multiplying each pressure with the tributary width of 6.125 feet. The values thus obtained are 653 kips per feet (On center stringer) and 388 kips per feet (adjacent stringers). These uniformly distributed loads were again converted into equivalent nodal loads. Finally, the nodal loads obtained are 6530 kips (center stringer) and 3880 kips (adjacent stringers).

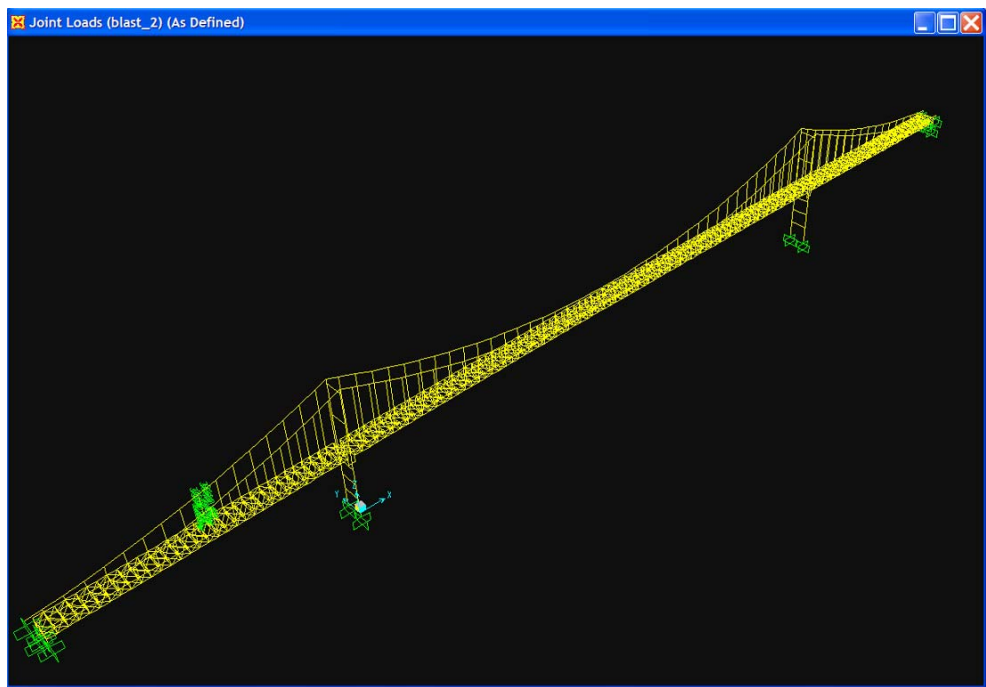


Figure 5.5: Application of Blast load at center of side-span

The axial load and the moment produced by these loads are presented in Figure 5.6 and Figure 5.7.

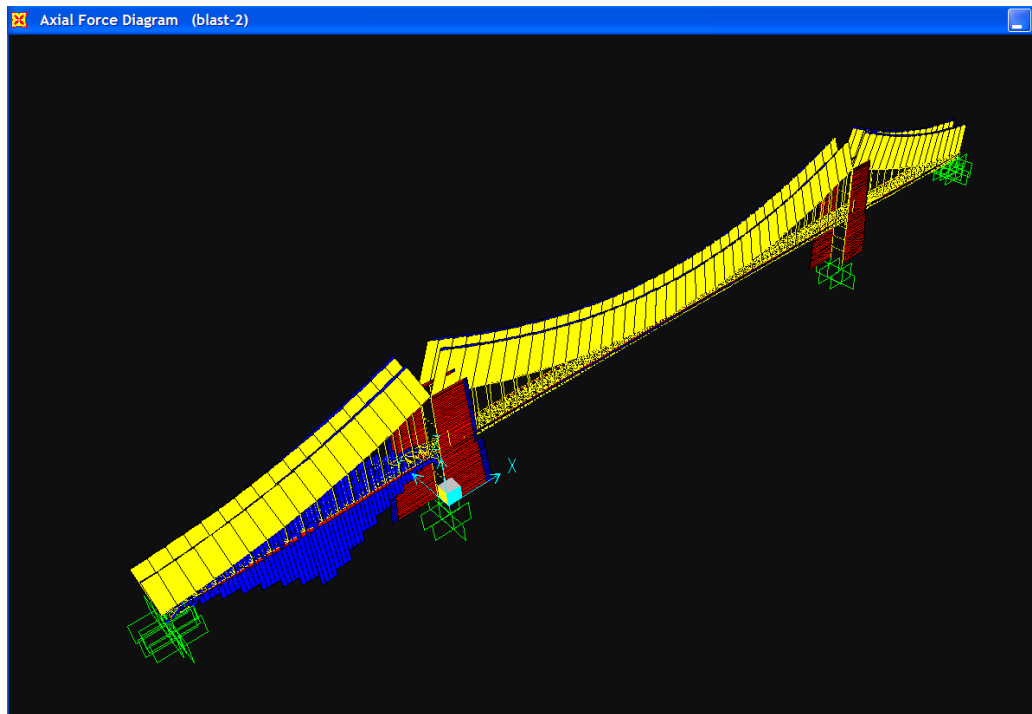


Figure 5.6: Axial force diagram for blast load case 2

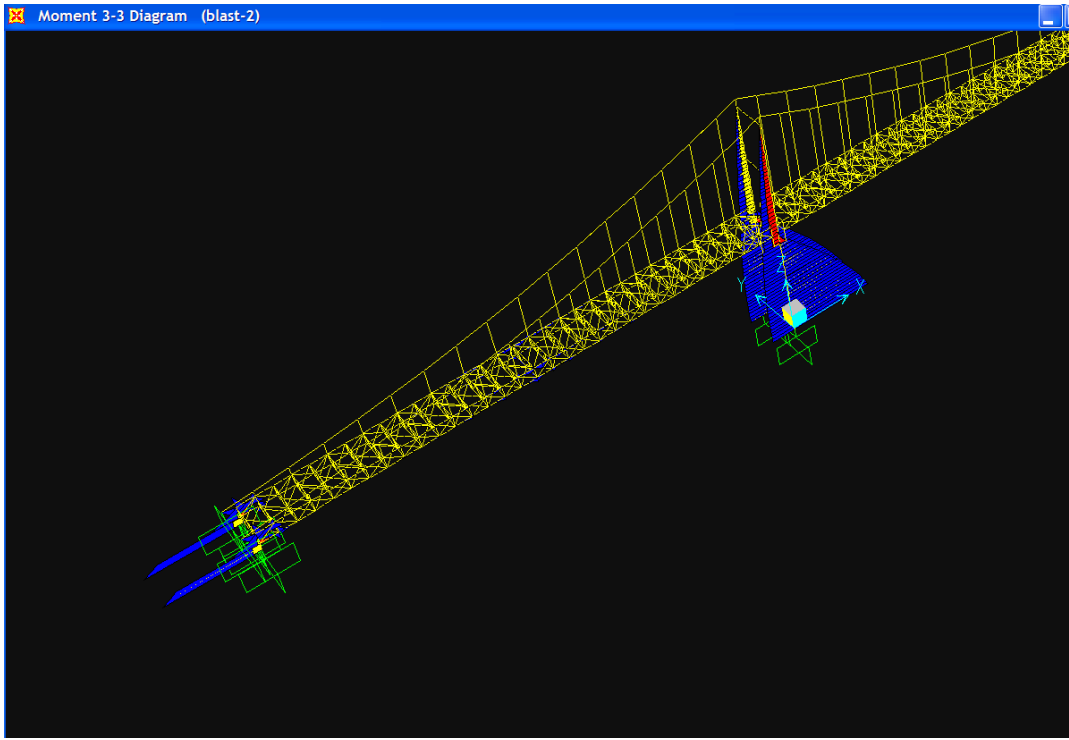


Figure 5.7: Bending moment diagram on tower for blast load case 2

5.3 Load Combination 3

As shown in Figure 5.8, this load combination was defined to take place at the end, near the tower of the mid span at 6 feet above the deck. Similar to load combination 1, the nodal loads obtained are 6530 kips (center stringer) and 3880 kips (adjacent stringers).

The axial load and the bending moment diagrams are shown in Figure 5.9 and Figure 5.10 respectively.

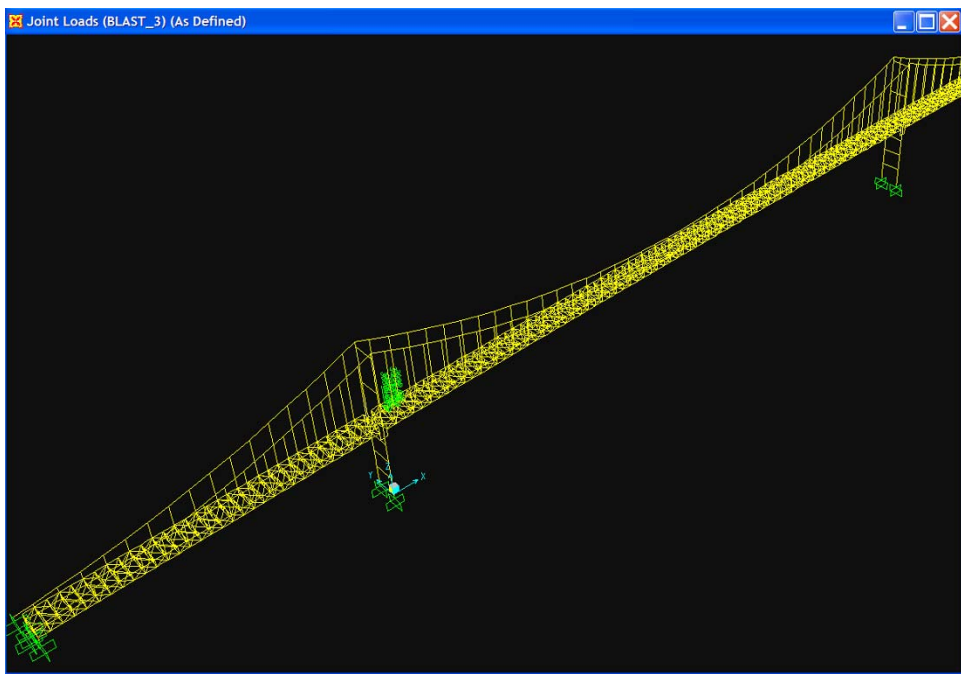


Figure 5.8. Application of Blast load at end of mid-span

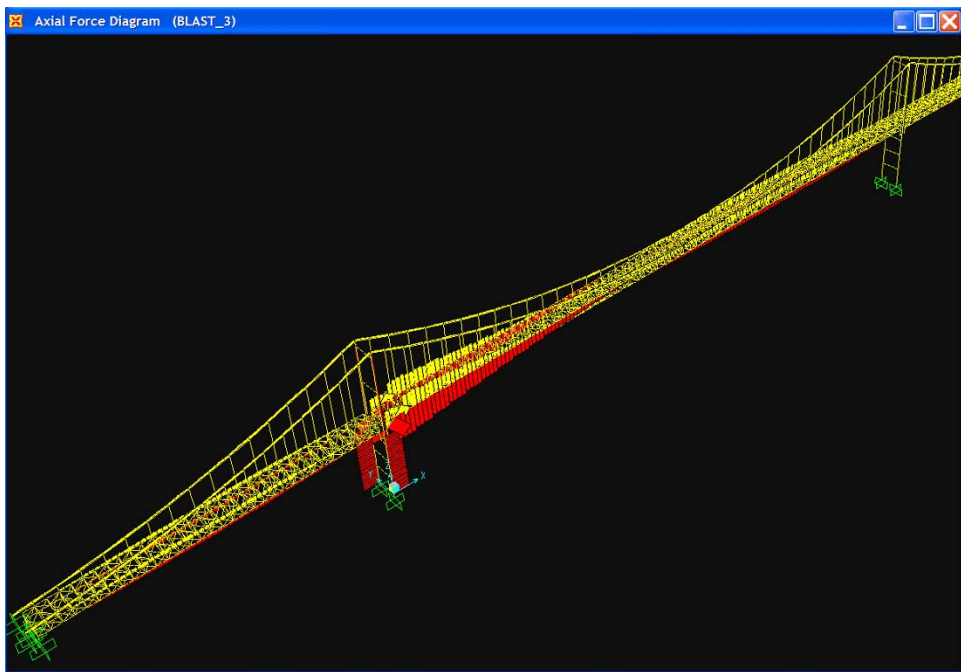


Figure 5.9. Axial load diagram for blast load case 3

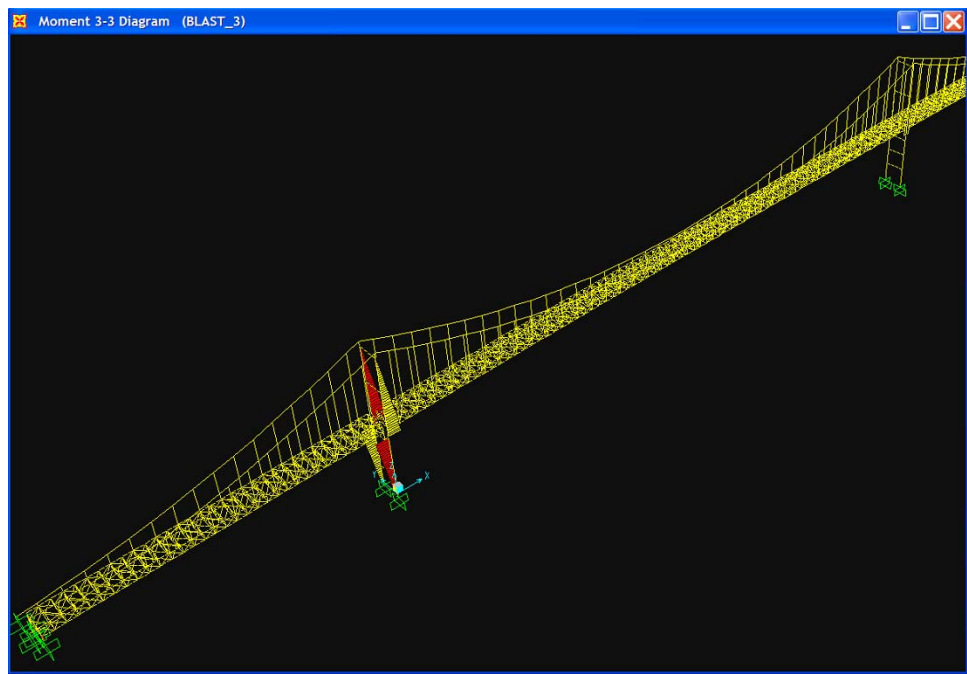


Figure 5.10. Bending moment diagram for load case 3

5.4 Progressive Collapse

Local failure of a structural element may cause failure of other elements of the same structure. In this way, entire structure may be affected by a localized failure. Different structures may have different sensitivity towards progressive collapse. While considering the typical design of any structure the concept of progressive collapse is not exactly implemented. This means that we are just designing for the safety of a particular member rather than the safety of the entire structure.

Current design codes do not strictly require the prevention of progressive collapse. Recent disasters and theoretical consideration on the basis of risk theory indicates that codes should be improved to more clearly address this problem.

To carry out the progressive collapse analysis, the computer program should be capable of instantaneous change in the stiffness matrix and geometry. Very few computer programs are capable of doing this, and those that are available are discouragingly

expensive. The key issue in the progressive collapse understands the dynamic behavior and the release of internal energy due to instantaneous loss of structural member. This member loss disturbs the initial load equilibrium of external loads and internal forces, and the structure then degrades until a new equilibrium position is found or until the structure collapses.

In the suspension bridge, the plastic hinges are assigned to the top and bottom chord of the main truss near the application of the blast load at location 1, which is in the centre of the mid-span. The static non-linear analysis is carried out using SAP2000 software. The progressive formation of the plastic hinges with the application of the stage loading can be obtained. This gives a clear idea about the flow of internal energy due to sudden breakdown of one member. Figure 5.8 shows the formation of plastic hinges with the application of the stage loading, step 1.

When the structure is subjected to a large force and/or moment that vary with the time, a particular state of lateral deformation will exist in the structure, and at some time within the period in which the structure is responding to this motion to attain stability, a maximum pattern of deformation will occur. At relatively low level of structure motion the deformation induced within the structure will be limited and resulting stresses that develop within the structural components will be within the elastic limit. Within this limit the structure will experience no damage. The structural component will retain its original strength, stiffness and appearance.

At more severe levels of force, the lateral deformations induced into the structure will be larger. As these deformations increase, so will demands on the individual structural components. At different levels of normalized force, component of the structure will be strained beyond its elastic limit. At this stage, individual component might experience damage in the form of cracking, spalling, buckling and yielding of various other components. As components become damaged, they degrade in stiffness and some elements will begin to lose strength. Some permanent deformation may remain in the structure permanently and damage will be evident throughout.

At the Immediate Occupancy level, damage is relatively limited. The structure retains a significant portion of its original stiffness and most if not all of its strength. At Collapse prevention level, the structure has experienced extreme damage. At life safety level, substantial damage has occurred to the structure and it may have lost a significant amount of its original stiffness. However, a substantial margin remains for additional lateral deformation before the collapse would occur.

The plastic hinges were applied on the top and bottom chord members that are very near to the application of blast, and hence have maximum deformation. These members now undergo plastic deformations. Figure 5.12 gives a clear picture for the limits that are set for the three performance levels. Figures 5.13 through 5.28 give the formation of different hinges depending upon the stage loading. This stage loading, also known as step loading is summarized in Table 5.2 where P is the axial force, $UIPl$ is the plastic deformation, $UIPl \text{ max}$ and $UIPl \text{ min}$ are the maximum and minimum deformations in, $U1state$ is the hinge state and the $U1stage$ is the performance stage (immediate occupancy, life safety or collapse prevention). Table 5.2 is also graphically represented in Figures 5.29 through 5.32.

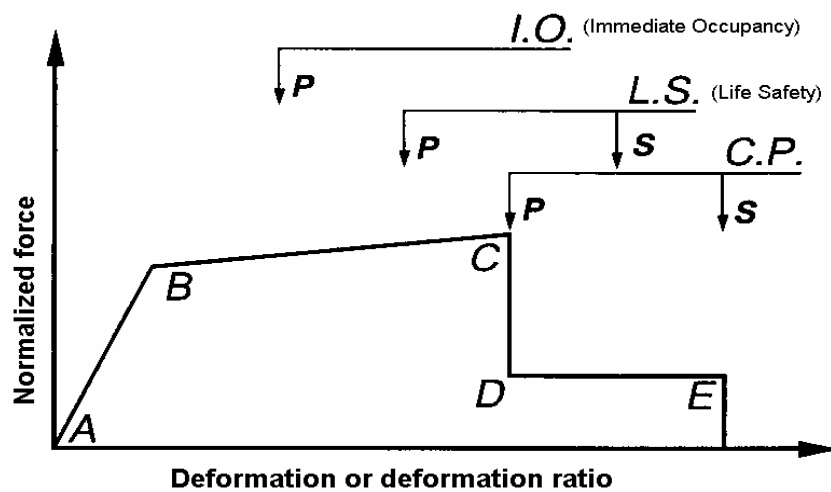


Figure 5.11: Curve showing relationship between the force and the deformation (Step 1)

Step	P	U1Pl	U1PlMax	U1PlMin	U1State	U1Status
	(Kip)	(in)	(in)	(in)		
0	863.006	0	0	0	A ≤ B	A ≤ IO
1	1941.219	0	0	0	A ≤ B	A ≤ IO
2	1979.023	0	0	0	A ≤ B	A ≤ IO
3	-196.29	0	0	0	A ≤ B	A ≤ IO
4	-607.672	0	0	0	A ≤ B	A ≤ IO
5	-889.536	0	0	0	A ≤ B	A ≤ IO
6	-946.447	0	0	0	A ≤ B	A ≤ IO
7	-884.985	0	0	0	A ≤ B	A ≤ IO
8	-1575.105	0	0	0	A ≤ B	A ≤ IO
9	-2795.405	-0.007607	0	-0.007607	B ≤ C	A ≤ IO
10	-3138.39	-0.440825	0	-0.440825	B ≤ C	IO ≤ LS
11	-3426.808	-0.805119	0	-0.805119	B ≤ C	LS ≤ CP
12	-3443.633	-0.82637	0	-0.82637	B ≤ C	LS ≤ CP
13	-0.034	-1.174431	0	-1.174431	> E	> CP
14	-0.034	-1.174431	0	-1.174431	> E	> CP
15	-0.034	-1.174431	0	-1.174431	> E	> CP
16	-0.034	-1.174431	0	-1.174431	> E	> CP
17	-0.034	-1.174431	0	-1.174431	> E	> CP

Table 5.2: Results for Plastic hinge located at node 942

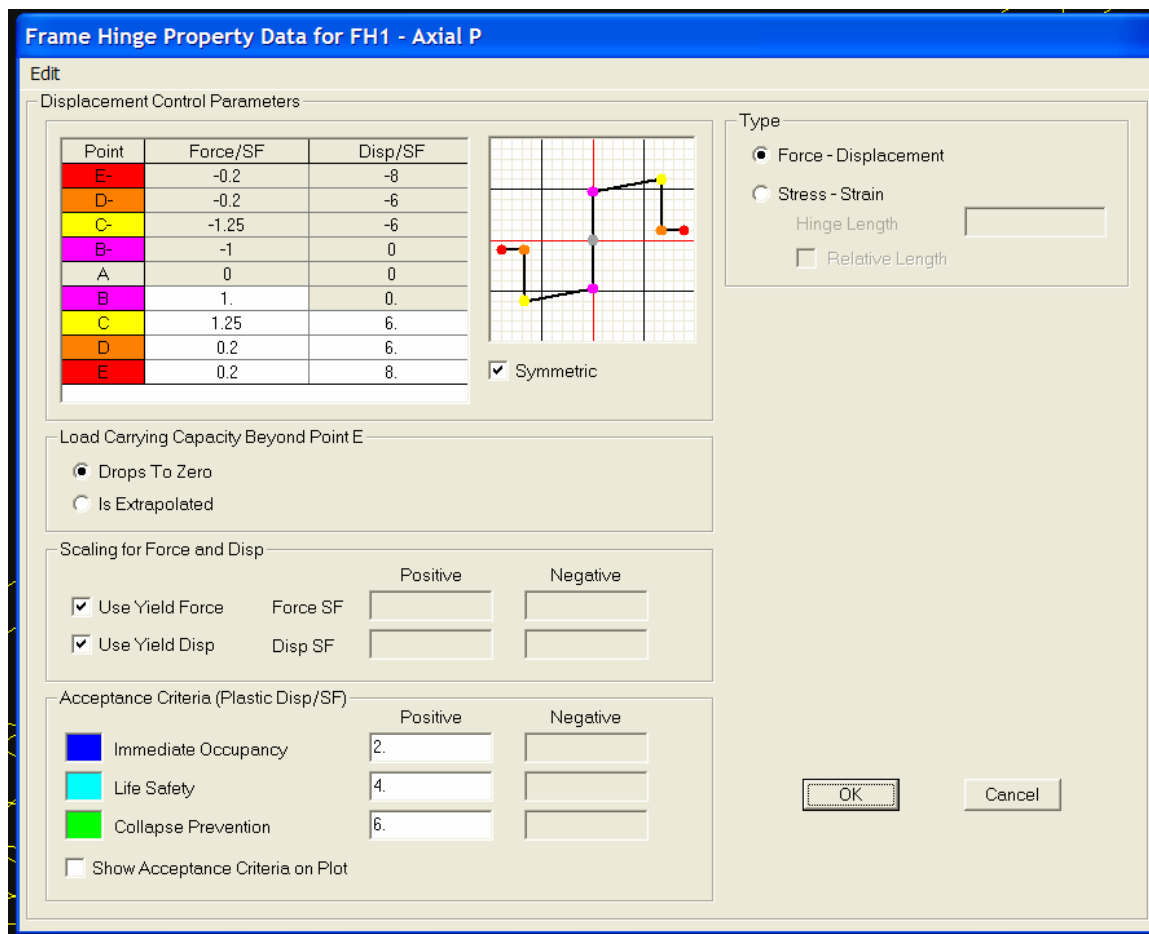


Figure 5.12 Plastic Hinge properties in SAP2000

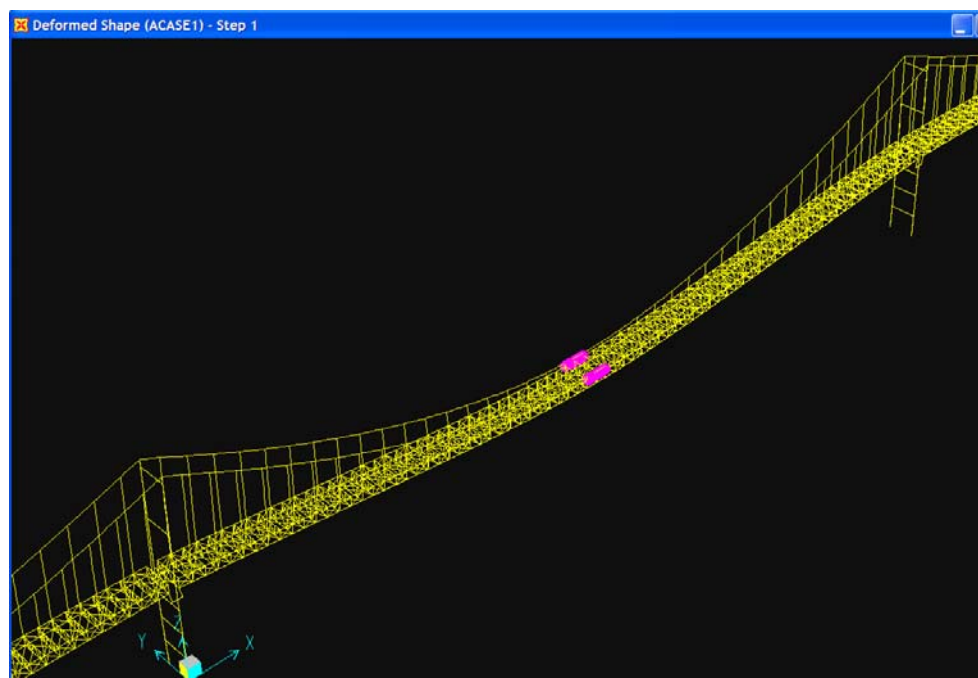


Figure 5.13 Formation of plastic hinges due to blast load 1 (Step 1)



Figure 5.14 Formation of plastic hinges due to blast load 1 (Step 1)

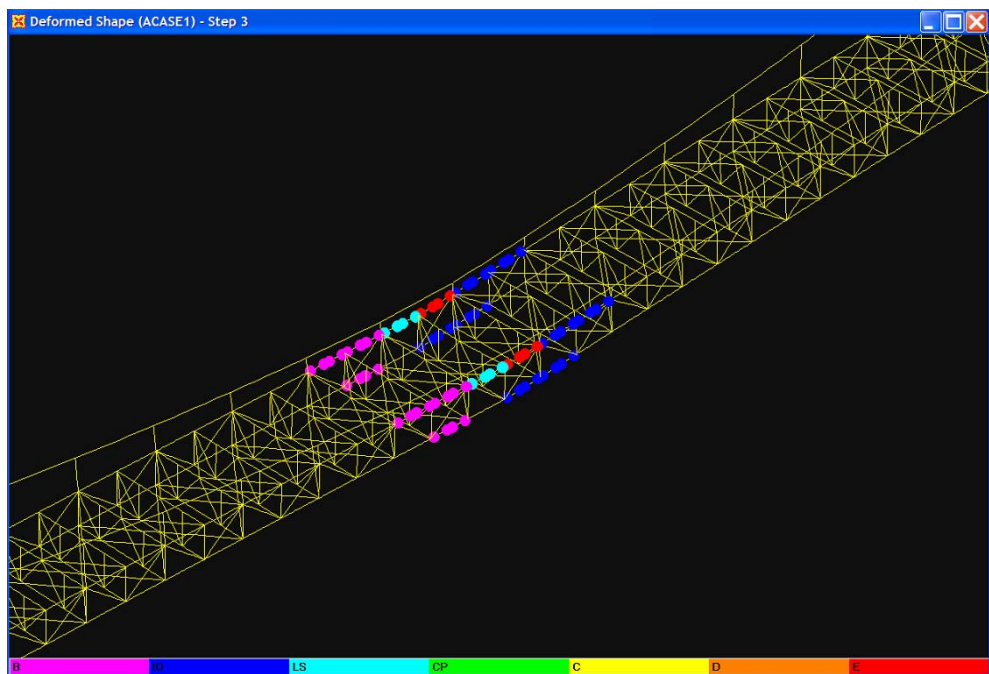


Figure 5.15 Formation of Plastic Hinges due to blast load 1 (Step 3)

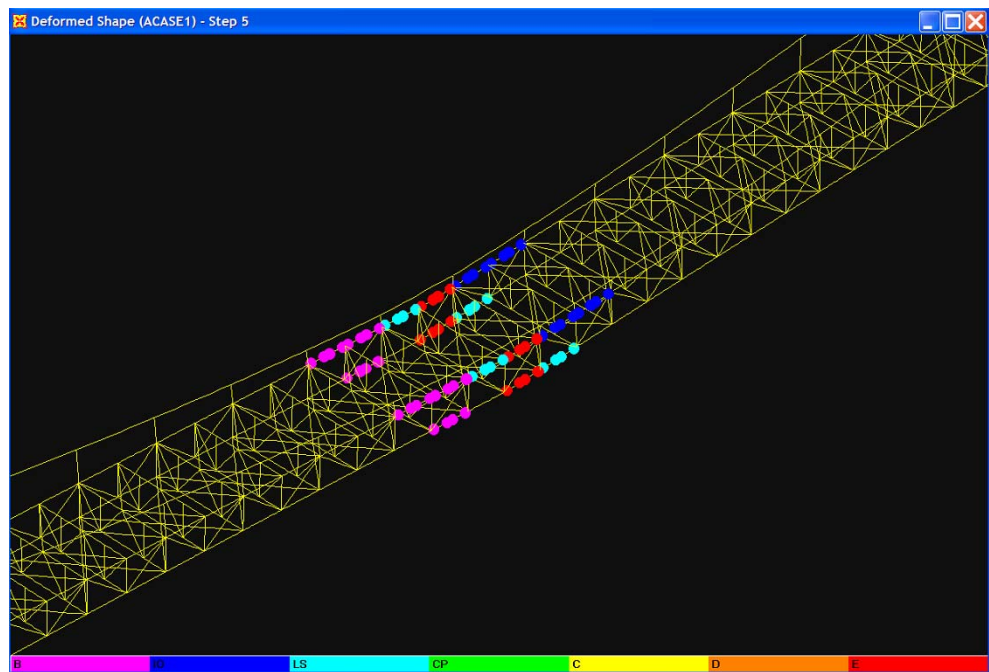


Figure 5.16 Formation of plastic hinges due to blast load 1 (Step 5)

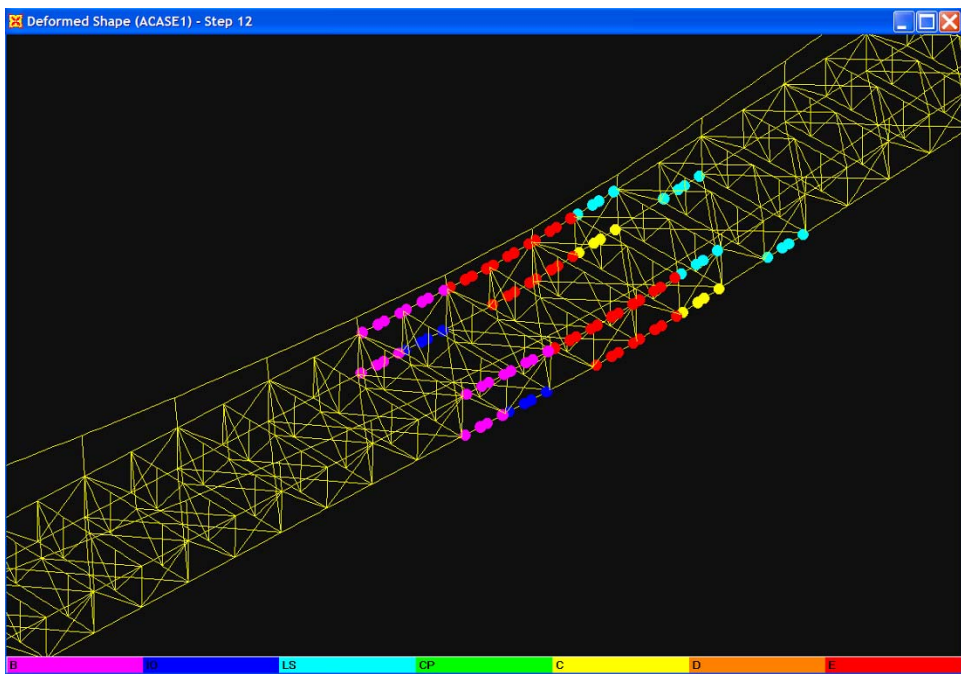


Figure 5.17 Formation of plastic hinges due to blast load 1 (Step 12)

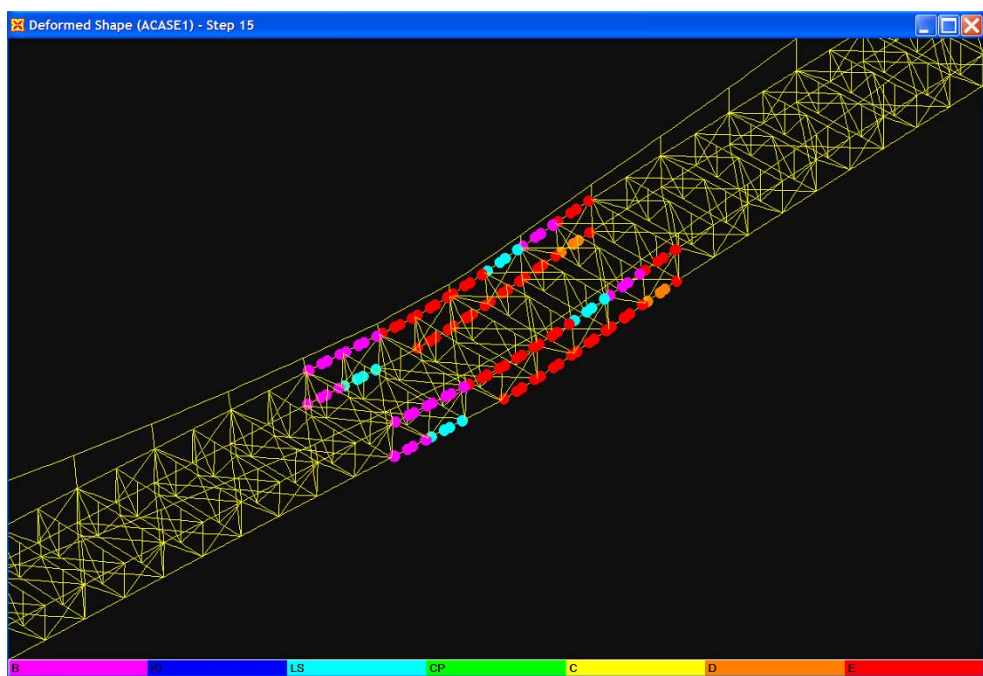


Figure 5.18 Formation of plastic hinges due to blast load 1 (Step 15)



Figure 5.19 Formation of plastic hinges due to blast load 2 (Step 1)



Figure 5.20 Formation of plastic hinges due to blast load 2 (Step 5)



Figure 5.21 Formation of plastic hinges due to blast load 2 (Step 11)



Figure 5.22 Formation of plastic hinges due to blast load 3 (Step 1)



Figure 5.23 Formation of plastic hinges due to blast load 3 (Step 5)



Figure 5.24 Formation of plastic hinges due to blast load 3 (Step 10)

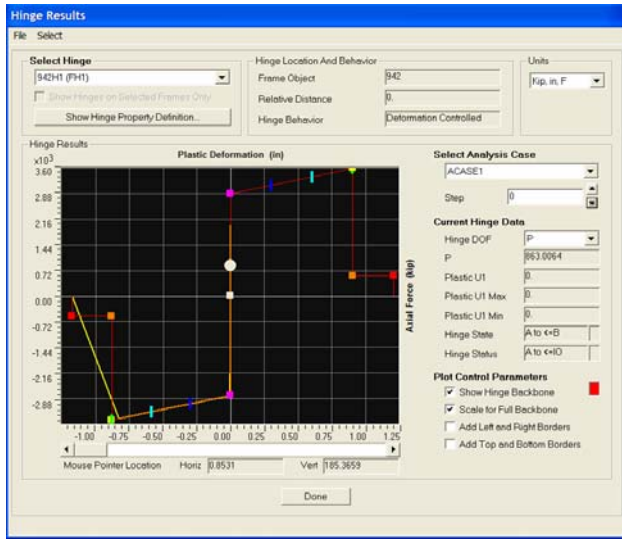


Figure 5.25 Relation between Plastic deformation Vs Axial force (Step 0)

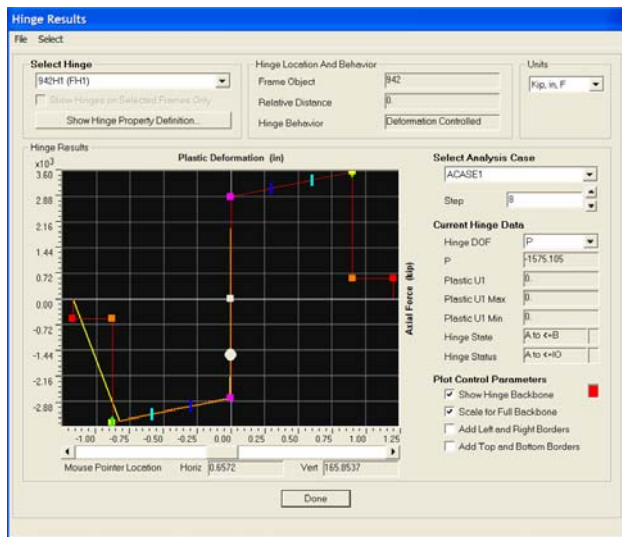


Figure 5.26 Relation between Plastic deformations Vs Axial force (Step 8)

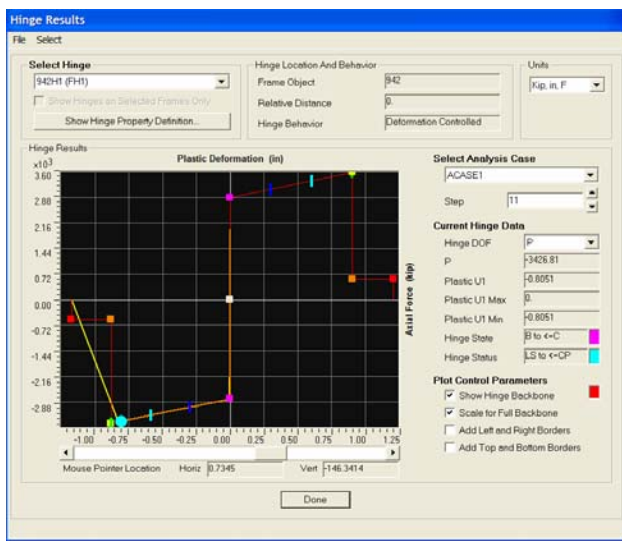


Figure 5.27 Relation between Plastic deformation Vs Axial force (Step 11)

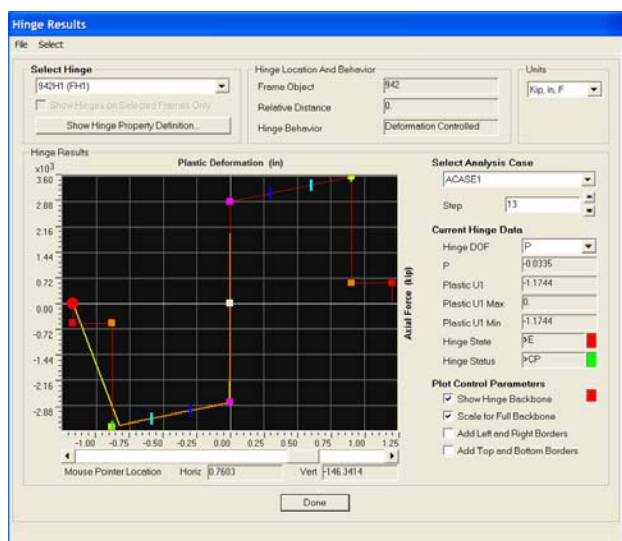


Figure 5.28 Relation between Plastic deformation Vs Axial force (Step 13)

5.5. Summary of Results

DEFLECTION DUE TO LIVE LOAD WITH INITIAL STRESS	DEFLECTION DUE TO LIVE LOAD WITHOUT INITIAL STRESS
78 in	230 in

Table 5.3. Effects of the initial stress on the deflection of the bridge.

BLAST LOAD CASE	MAX VERTICAL DISPLACEMENT (in)
CASE 1	540.27 in
CASE 2	287.69 in
CASE 3	340.21 in

**Table 5.4. Max vertical displacements due to application of blast loads combination
(1.25DL + 0.5LL + 1.0BLAST)**

6. CONCLUSION

1. Firstly, it should be mentioned that the suspension bridge is a “signature” facility and should be designed for security. Operating security measures are in place and employed by bridge owners who operate “signature” facilities. Also site improvement and operation procedures will often prove to be more cost effective than structural engineering solutions.
2. Research is needed to assess structural responses and to validate and calibrate methods and models. Structural engineering guidance needs to be developed by expanding on work by DOD and AASHTO/FHWA Blue Ribbon Panel (BRP) through research leading to design guidance.
3. This model is a typical suspension bridge with assumptions to make the analysis simpler. It is performed purely for the illustrative purposes and should not be taken as indicator for any kind of terrorist attack. Assumptions were made on the blast load and its locations. Also the standoff distance plays an important role in protection of the members against the blast.
4. The dead and live load results from finite element software SAP2000 were in close proximity with that of VBDS software, which was used in the cost allocation study. The blast load analysis when carried out in SAP2000 will basically allow the researcher to determine the effect of blast on a suspension bridge under nonlinear analysis.
5. To simulate the blast load, the results were based on the equivalent static load rather than the dynamic loading on the suspension bridge. A numerical model that was created using SAP2000 finite-element-analysis software considering material and geometric nonlinearity.
6. Three blast load cases at the middles of central span and end span and also near the tower were investigated. These three blast load cases that were taken into account reveals the local failure (plastic hinges formation) of the members.
7. The blast load cases that were applied at the centre of the spans (blast load case 1 and 2) had more severe effect than that of blast that was applied near the tower (blast load case 3). However, the third blast load case is critical due to its closeness to the tower.
8. Suspension bridge is a highly redundant structure due to its multi-cell tower sections, multi-strand cables and hangers, and truss sections. It is also concluded from the analytical results that the bridge suffered a local failure, but not a global failure, under the application of blast loads.
9. From progressive collapse results, it can be concluded that parts of the bridge members failed due to application of blast loading, especially those which were

directly under the blast load applications. The plastic hinges that were formed on the top and bottom chord of the members just below the blast loads could be considered in a performance state of “collapse prevention”, but the performance level was “life safety” and even “immediate occupancy” for members away from the blast load.

10. This research only demonstrates the vehicular-bound blast load cases on the deck of a suspension bridge. Further research should be done on different blast loads at different locations on a random basis.

APPENDIX

Section A- Structural Analysis Assumptions and Property Assignments

Material

Carbon (A36 or A529) – Pylons, Part of main trusses and others if not specified

$$E = 29,000 \text{ ksi } (4,176,000 \text{ kips}/\text{ft}^2)$$

$$G = 11,000 \text{ ksi } (1,584,000 \text{ kips}/\text{ft}^2)$$

$$u = 0.3$$

$$\text{Alfa (thermal)} = 6.5 \times 10^{-6}/^\circ\text{F}$$

$$\text{Gama (Density)} = 0.49 \text{ kips}/\text{ft}^3$$

VBDS material number - 202

Low Alloy (A572) – Part of main trusses

Same as carbon steel except the yielding strength

Section Number

1 – Tower legs (Tier 1)

2 – Tower legs (Tier 2)

...

9 – Tower legs (Tier 9)

10 – Linkages

11 – Intermediate Struts

12 – Roadway Struts

13 – Top Struts

14 – Top chord U0-U3, U29-U36

Bottom chord L30-L32

2 Web Plates 15" x 13/16" and 2 Cover Plates 17" x 1/2"

Axial Area: 41.375 si

Iy (transverse bending): 2007.5 qi

Iz (vertical bending): 1478.5 qi

Ix (torsional constant): 2447.1 qi

Weight Area: Axial Area + equivalence area of node plates =

$$41.375 + (71+61.31)/2/(20 \times 12)/0.283 =$$

41.375 + 1 si = 42.375 si (increase the axial area by one square inch to consider the weight of node plates)

15 – Top chord U3-U9, U23-U29, U40-U58

2 Web Plates 15" x 1 7/8" and 2 Cover Plates 16" x 1/2"

Axial Area: 72.25 si

Iy (transverse bending): 3151.1 qi

Iz (vertical bending): 2012.4 qi

Ix (torsional constant): 2694.6 qi

Weight Area: 73.25 si

- 16 – Top chord U9-U11, U21-U23, U58-U62
 Bottom chord L39-L47, L51-L59
 2 Web Plates 15"x2" and 2 Cover Plates 16"x1/2"
 Axial Area: 76.0 si
 I_y (transverse bending): 3287.3 qi
 I_z (vertical bending): 2082.5 qi
 I_x (torsional constant): 22718.2 qi
 Weight Area: 77.0 si
- 17 – Top chord U11-U13, U19-U21, U62-U72
 Bottom chord L4-L8, L24-L28, L47-L51, L63-L73
 2 Web Plates 15"x2 1/8" and 2 Cover Plates 16"x1/2"
 Axial Area: 79.75 si
 I_y (transverse bending): 3417.87 qi
 I_z (vertical bending): 2152.53 qi
 I_x (torsional constant): 2739.95 qi
 Weight Area: 80.75 si
- 18 – Top chord U13-U19
 Bottom chord L59-L63
 2 Web Plates 15"x2 1/4" and 2 Cover Plates 15"x1/2"
 Axial Area: 82.5 si
 I_y (transverse bending): 3036 qi
 I_z (vertical bending): 2162 qi
 I_x (torsional constant): 2530 qi
 Weight Area: 83.5 si
- 19 – Top chord U36-U40
 2 Web Plates 15"x1 5/8" and 2 Cover Plates 16"x1/2"
 Axial Area: 64.75 si
 I_y (transverse bending): 2861.0 qi
 I_z (vertical bending): 1872.25 qi
 I_x (torsional constant): 2638.8 qi
 Weight Area: 65.75 si
- 20 – Bottom chord L0-L4, L28-L30
 2 Web Plates 15"x1 1/4" and 2 Cover Plates 16 1/2"x1/2"
 Axial Area: 50.125 si
 I_y (transverse bending): 2309.6 qi
 I_z (vertical bending): 1614.5 qi
 I_x (torsional constant): 2871.0 qi
 Weight Area: 51.125 si
- 21 – Bottom chord L8-L10, L22-L24
 2 Web Plates 15"x2 1/2" and 2 Cover Plates 15"x1/2"

Axial Area: 90.0 si
Iy (transverse bending): 3230.5 qi
Iz (vertical bending): 2302.7 qi
Ix (torsional constant): 2568.9 qi
Weight Area: 91.0 si

22 – Bottom chord L10-L12, L20-L22
2 Web Plates 15"x2 3/4" and 2 Cover Plates 15"x1/2"
Axial Area: 97.5 si
Iy (transverse bending): 3405.1 qi
Iz (vertical bending): 2442.8 qi
Ix (torsional constant): 2608.6 qi
Weight Area: 98.5 si

23 – Bottom chord L12-L20
2 Web Plates 15"x3" and 2 Cover Plates 15"x1/2"
Axial Area: 105.0 si
Iy (transverse bending): 3588.75.1 qi
Iz (vertical bending): 2588.75 qi
Ix (torsional constant): 2076.1 qi
Weight Area: 106.0 si

24 – Bottom chord L33-L37
2 Web Plates 15"x1 1/8" and 2 Cover Plates 16 1/2"x1/2"
Axial Area: 50.25 si
Iy (transverse bending): 2367.58.1 qi
Iz (vertical bending): 1622 qi
Ix (torsional constant): 2566.9 qi
Weight Area: 51.25 si

25 – Bottom chord L37-L39
2 Web Plates 15"x1 3/4" and 2 Cover Plates 16"x1/2"
Axial Area: 68.5 si
Iy (transverse bending): 1942.3 qi
Iz (vertical bending): 3009 qi
Ix (torsional constant): 2668.4 qi
Weight Area: 69.5 si

26 – 18WF96
Diagonals L0-U9, U23-L32, L33-U36
Axial Area: 28.5 si
Iy (transverse bending): 1750 qi
Iz (bending in main truss plane): 201 qi
Ix (torsional constant): 5.86 qi
Weight Area: 28.5 si (no extra weight on all diagonals and verticals)

27 – 18WF77

Diagonals U9-U23, U36-U72

All Verticals

Axial Area: 22.3 si

Iy (transverse bending): 1330 qi

Iz (bending in main truss plane): 152 qi

Ix (torsional constant): 2.83 qi

Weight Area: 22.3 si (no extra weight on all diagonals and verticals)

28 – Hangers

4 x 1 5/8" Ø

Axial Area: 8.296 si

Weight Area: 8.296 si (no extra weight on all hangers)

29 – Cables

3577 x 0.198" Ø

Axial Area: 110.14 si

Weight Area: 111.14 si (approximately 1 si for hand rope)

30 – Lateral Diagonal Bracings (14WF61)

Axial Area: 17.9 si

Iy (transverse bending): 107 qi

Iz (vertical bending): 640 qi

Ix (torsional constant): 2.19 qi

Weight Area: 17.9 si (no extra weight on all lateral bracings)

31 – Top Chord of Floor Beam Truss at Ends (U0, U32 and U33) (U32 and U33 are assumed as the same as U0). (2-13" X 4" X 31.8 channels, 13 1/8" spacing, with top and bottom cover plates of 19" X 7/16", ignoring perforations)

Axial Area: 35.33 si

Iy (transverse bending): 1313 qi

Iz (vertical bending): 1228 qi

Ix (torsional constant): 918 qi

Weight Area: $35.33 + 4000 * 20 / 490 * 12 * 12 * 12 / 49 / 12 = 35.33 + 479.8 =$

515.13 si (deck weight is 4000lb/ft, the total length of floor beam is 49 ft)

32 – Top Chord of Floor Beam Truss at all internals (same as 31 except the space between two channels is 11 1/8")

Axial Area: 35.33 si

Iy (transverse bending): 1313 qi

Iz (vertical bending): 1228 qi

Ix (torsional constant): 918 qi

Weight Area: $35.33 + 4000 * 20 / 490 * 12 * 12 * 12 / 49 / 12 = 35.33 + 479.8 =$

515.13 si (deck weight is 4000lb/ft, the total length of floor beam is 49 ft)

33 – Bottom Chord of Floor Beam Truss at Ends (L0, L32 and L33) (L32 and L33 are assumed as the same as L0). (Same channels as 31 with a spacing of 13 1/8, no cover plates, stay plates are all assumed as 19 1/8" X 3/8" X 1'-8". Stay plates ignored in stiffness but its weight, 20 stay plates totally in one bottom beam).

Axial Area: 18.82 si

Iy (transverse bending): 836.32 qi

Iz (vertical bending): 465.87 qi

Ix (torsional constant): 1.635 qi

Weight Area: $18.82 + 20 * 21 \frac{1}{8} * \frac{3}{8} * 20 / 49/12 = 18.82 + 5.4 = 24.2$ si

34 – Bottom Chord of Floor Beam Truss at all internals (same as 33 except the space between two channels is 11 1/8")

Axial Area: 18.82 si

Iy (transverse bending): 836.32 qi

Iz (vertical bending): 465.87 qi

Ix (torsional constant): 1.635 qi

Weight Area: $18.82 + 20 * 21 \frac{1}{8} * \frac{3}{8} * 20 / 49/12 = 18.82 + 5.4 = 24.2$ si

35 – Vertical and Diagonal Members of Floor Beam Truss at Ends (0, 32 and 33) 32 and 33 are assumed as the same as 0) – 12WF45.

Axial Area: 13.1 si

Iy (transverse bending): 348 qi

Iz (vertical bending): 50 qi

Ix (torsional constant): 1.26 qi

Weight Area: 13.1 si (no extra weight on all diagonals and verticals)

36 – Vertical and Diagonal Members of Floor Beam Truss at all internals – 10WF39.

Axial Area: 11.5 si

Iy (transverse bending): 209 qi

Iz (vertical bending): 45 qi

Ix (torsional constant): 0.976 qi

Weight Area: 11.5 si (no extra weight on all diagonals and verticals)

37 – Wind Tongues at Tower (2 – 11 1/2" x 1" Flange Plates + 2'10"x2" Web Plate). The modeling length of tongues at tower is 3'7" (sheet 134). The effective length is 2'7" (connected at quarter of roadway strut as assumed, rather than at the center of the strut). Bending inertia is both directions will be adjusted as follows due to the difference between the modeling length and effective length,

$$I_e = \left(\frac{l_m}{l_e} \right)^3 I = \left(\frac{3'7"}{2'7"} \right)^3 I = 19I \approx 20I$$

i.e. the tongue's inertia in both directions will be increased 20 times to simulate the enhancement of shear stiffness due to the rigidness of roadway strut.

Axial Area: 93 si

Iy (transverse bending): 271920 qi

Iz (vertical bending): 7869.4 qi

I_x (torsional constant): 101 qi
Weight Area: 93 si

38 – Wind Tongues at Anchors. (27WF177, the modeling length is assumed as $2' - 3 \frac{5}{6}'' + 1' - 4 \frac{1}{2}'' / 2 = 3'$, see sheet 131. No need to adjust its inertia.)

Axial Area: 52.5 si
 I_y (transverse bending): 7020 qi
 I_z (vertical bending): 555 qi
 I_x (torsional constant): 20.1 qi
Weight Area: 52.5 si

100 – Rigid bodies (connections between linkage and tower leg, bottom of saddles, bearings, no mass)

101 – Partial Rigid bodies (connections between cable and the bottom of saddles, no longitudinal bending stiffness to simulate free movement of cables over saddles, no mass)

Reference vector number

- 0 – (0,0,1) as local Z axis
 - All tower legs and main truss chords, linkage and its rigid body, wind tongues.
- 1 – (0,1,0) as local Y axis
 - All top and bottom bracings.
- 2 – (-1,0,0) as local Z axis
 - All tower struts, floor beam trusses (top and bottom chords, vertical and diagonal members)

REFERENCES

1. AASHTO LRFD bridge design specification, Washington D.C., 2003.
2. AASHTO/FHWA. Blue Ribbon Panel on Bridge and Tunnel Security,
Recommendations for Bridge and Tunnel Security. 2003
[<http://security.transportation.org/sites/security/brpt/brp.pdf>](http://security.transportation.org/sites/security/brpt/brp.pdf).
3. Winget, D.G., Marchand k.A. and Williamson E.B., "Analysis and design of critical bridges subjected to blast loads," Journal of Structural Engineering, ASCE, Vol. 131, No.8, August 1, 2005.
4. Benzi, M.T., "Generalized Assessment of bridge vulnerability to terrorist Threats, A probabilistic structural Analysis based approach," University of Delaware, 2006
5. Islam, A.K.M. Anwarul, "Performance of AASHTO girder bridges under blast loading.", Ph.D. dissertation, Florida State University, Tallahassee, FL, 2005.
6. TM-5-1300, "Structures to resist the effect of accidental explosions" US department of defense, Dec. 1990.
7. Bounds, W., ed, "Concrete and blast effects." Special publications SP-175, American concrete institute, Farmington Hills, Mich, 1998.
8. Starossek, U. and Sauvagot, G., Discussion on "Bridge progressive collapse vulnerability.", Journal of Structural Engineering, ASCE, Vol. 124, No. 12, 1998, pp. 1497-1498.
9. Starossek, U., "A progressive collapse of multi-span bridges- A case study", Structural engineering international, International Association for Bridge and Structural Engineering, Vol. 9, No. 2, 1999
10. Marjanishvili, S. and Agnew, E., "Comparison of various procedures for progressive collapse analysis," Journal of performance of constructed facilities, ASCE, Vol. 20, No.4, Nov 1, 2006.
11. Steinman, D.B, "Practical treatise on suspension bridges, their design, construction and erection,", 2nd edition, Wiley, 1929
12. Steinman, D.B, "Suspension bridges and cantilevers, their economic proportions and limiting spans," D. Van Nostrand Company, New York, 1911

13. Pugsley, A., "The theory of Suspension Bridge," Edward Arnold, 1957